

Design And Testing Of A Passive Prosthetic Ankle With Mechanical Performance Similar To That Of A Natural Ankle

Yadan Zeng
Marquette University

Recommended Citation

Zeng, Yadan, "Design And Testing Of A Passive Prosthetic Ankle With Mechanical Performance Similar To That Of A Natural Ankle" (2013). *Master's Theses (2009 -)*. Paper 188.
http://epublications.marquette.edu/theses_open/188

DESIGN AND TESTING OF A PASSIVE PROSTHETIC ANKLE
WITH MECHANICAL PERFORMANCE SIMILAR TO
THAT OF A NATURAL ANKLE

by

Yadan Zeng, B.S.

A Thesis Submitted to the Faculty of the Graduate School,
Marquette University,
In Partial Fulfillment of the Requirements for
The Degree of Master of Science

Milwaukee, Wisconsin
May 2013

ABSTRACT

DESIGN AND TESTING OF A PASSIVE PROSTHETIC ANKLE WITH MECHANICAL PERFORMANCE SIMILAR TO THAT OF A NATURAL ANKLE

Yadan Zeng, B.A.

Marquette University, 2012

This thesis presents the design and test results of a passive prosthetic ankle that has mechanical behavior similar to that of a natural ankle. The ankle prosthesis is designed to store and return enough energy to the amputee to propel their body forward during push-off.

The ankle prosthesis is a 2 degree of freedom (DoF) mechanism containing a network of conventional compression springs. One DoF allows the lower leg to compress when weight is applied; the other allows the foot to rotate about the ankle joint. Bulk property and dynamic performance criteria are used to assess the performance of the ankle prosthesis. Lightweight, compactness and low friction are the primary bulk property requirements for the ankle device. Stiffness nonlinearity and active behavior similar to that of a human ankle are the major dynamic performance characteristics.

In this research, a preliminary computer geometric model of the prosthesis was developed, simulated, and refined in CAD software. A proof-of-concept prototype was then fabricated, modified and tested on both a robot and a human subject. The test results showed that the designed ankle prosthesis demonstrated its ability to satisfy the bulk property requirements and some of the dynamic performance characteristics. The nonlinearity of ankle stiffness was validated, however, more active behavior should be achieved by the prosthesis during push-off.

ACKNOWLEDGEMENTS

Yadan Zeng, B.S.

I would first like to acknowledge my advisor Dr. Joseph M. Schimmels, for giving me the opportunity to take this research and for all the guidelines and financial assistance. I would want to thank Dr. Shuguang Huang for giving me a theoretical insight of this work and many critical suggestions. I would thank Dr. Phillip A. Voglewede for introducing me to this work and opening his lab to me. I also thank Jinming Sun, Brian Slaboch, Fernando Rodriguez Anton and Jacob Rice for their support and help in the lab. I also thank Tom Current and Jessica Fritz for their working during the human subject test.

This work is supported by a grant from the National Institute of Health (*NIH*), grant No. 1R21EB006840 and more recently by NIDRR, grant No. H133G120256. An ATI 6-axis *F/T* Sensor that was used to measure the test results from robot was provided by Dr. Stango. I appreciate their support.

In addition, I would like to express my gratitude to my parents. Without their support and encouragement, I would not have finished this work.

TABLE OF CONTENTS

ACKNOWLEDGEMENTS	i
TABLE OF CONTENTS	ii
LIST OF FIGURES	v
CHAPTER 1 Introduction	1
1.1 Motivation	1
1.2 Normal Gait.....	2
1.2.1 Fundamental Analysis of Gait	3
1.2.2 Dynamic Analysis of Gait	5
1.3 Existing Ankle Prostheses.....	7
1.3.1 Passive Prostheses	8
1.3.2 Powered Prostheses	11
1.3.3 Summary.....	18
1.4 Goal of this Research	19
CHAPTER 2 Conceptual Design.....	19
2.1 Design Criteria	20
2.2 Design Strategies.....	22
2.2.1 Use of Conventional Passive Springs.....	22
2.2.2 Task 1: Obtain Nonlinear Stiffness	23
2.2.3 Task 2: Generate Adequate Torque at the Ankle	24
2.2.4 Task 3: Match the Natural Torque Profile.....	26
2.3 Conceptual Model of the Passive Ankle Prosthesis.....	26
2.4 Optimization Process and Results	30
CHAPTER 3 Structural Design and Component Selection.....	35
3.1 Main Structure Design	35

3.1.1	Structure Design in NX	36
3.1.2	Material Selection.....	39
3.2	Spring Selection and Spring Connection Design	39
3.2.1	Spring Selection.....	40
3.2.2	Design of Spring Connection Mechanisms	42
3.3	Design of Lock and Unlock Mechanism.....	44
3.4	Selection of Bearings and Other Conventional Components.....	47
3.5	Motion Simulation.....	48
3.6	Fabrication of the Ankle Prosthesis	49
CHAPTER 4	Ankle Performance Evaluation.....	51
4.1	Robot Testing.....	51
4.1.1	Robot Testing Configuration.....	51
4.1.2	Results and Analysis from Robot Tests.....	54
4.1.3	Conclusion.....	58
4.2	Human Subject Testing	59
4.2.1	Human Subject Test Method	59
4.2.2	Test Results and Analysis.....	59
4.2.3	Conclusion.....	63
CHAPTER 5	Conclusion and Future Work.....	65
5.1	Conclusion.....	65
5.2	Future Work	66
REFERENCE		68
APPENDIX A	Prosthetic Detailed Design Considerations	71
A.1	Prosthetic Mechanical and Material Properties.....	71
A.2	Prosthetic Fabrication Figures and Tables	74
APPENDIX B	Robot Testing Protocol and Results.....	77

B.1	Sensor Data Interpretation	77
B.2	Robot Testing Protocol for Designed Prosthesis	80
B.3	Robot Testing Results.....	81
APPENDIX C	Human Subject Testing Results	84

LIST OF FIGURES

Figure 1.1	Functional Division of a Gait Cycle for a Single Limb	3
Figure 1.2	Ankle Force, Torque and Angle Profiles from Dr. Winter [5].....	5
Figure 1.3	Torque-Angle Relationship from Dr. Winter [5]	6
Figure 1.4	Models of SACH Foot.....	9
Figure 1.5	ESAR Feet	10
Figure 1.6	CAD Model of SPARKy 3	12
Figure 1.7	Original PowerFoot One by iWALK Company [14]	13
Figure 1.8	PowerFoot One model [15]	14
Figure 1.9	Model of the four-bar prosthesis configuration. [16]	15
Figure 1.10	The Prototype of the Four-Bar Prosthesis [16].....	16
Figure 1.11	CESR Prosthesis [17]	17
Figure 2.1	Stiffness Nonlinearity: Stiffness changes as ankle angle deflects	23
Figure 2.2	Two sets of Unilateral Compression Springs	24
Figure 2.3	Spring Connection Geometry	25
Figure 2.4	Design of Bottom Springs with Different Free Lengths	26
Figure 2.5	Embodied Mechanical Model of the Prosthetic Ankle	27
Figure 2.6	Movements of Prosthetic Ankle during Stance Period.....	29
Figure 2.7	Torque Profile of the Prosthetic Ankle from Optimization.....	32
Figure 2.8	Torque-Angle Relationship of the Theoretical Prosthetic Ankle	33
Figure 3.1	NX Model for Upper-Leg A.....	36
Figure 3.2	NX Model for Lower-Leg B	37
Figure 3.3	NX Model for Foot C	38
Figure 3.4	Spring Mechanisms of ks_1 and ks_2/ks_3	43

Figure 3.5	Spring Mechanisms of k_1 and k_2	44
Figure 3.6	Locked Situation	45
Figure 3.7	Unlocked Situation.....	46
Figure 3.8	Representations of Motion Simulation Links.....	49
Figure 3.9	Modifications of the Prosthesis	49
Figure 4.1	Walking Trajectory of Human Fibular Joint.....	53
Figure 4.2	The Fully Assembled Prosthesis Mounted to the Robot with All Add-ons .	54
Figure 4.3	The Average Ankle Angle for Robot Test and Comparisons.....	55
Figure 4.4	The Average Ankle Torque for Robot Test and Comparisons.....	56
Figure 4.5	The Average Ankle Force for Robot Test and Comparisons	57
Figure 4.6	The Torque-Angle relationship for Robot Test and Comparisons	58
Figure 4.7	The Average Ankle Angle for Human Subject Test and Comparisons.....	60
Figure 4.8	The Average Ankle Force for Human Subject Test and Comparisons	61
Figure 4.9	The Average Ankle Torque for Human Subject Test and Comparisons.....	62
Figure 4.10	The Average Ankle Torque-Angle Relationship for Human Subject Test and Comparisons.....	63
Figure A.1.1	Spring Configurations for Spring Sets k_2 , k_{s1} and k_{s2}/k_{s3}	72
Figure B.1.1	Calibration curve for Linear Potentiometer	77
Figure B.1.2	Calibration Curve for Rotary Potentiometer.....	77
Figure B.1.3	Force and Torque Transformation of F/T Sensor	78
Figure B.1.4	Walking Trajectories of the Top Head of Fibula of a Natural Ankle	79
Figure B.1.5	The Ankle Angle Profiles for Each Robot Test Trial	81
Figure B.1.6	The Ankle Torque Profiles for Each Robot Test Trial	82
Figure B.1.7	The Ankle Force Profiles for Each Robot Test Trial.....	82
Figure B.1.8	The Torque-Angle Relationship Profiles for Each Robot Test Trial.....	83
Figure C.1.1	The Ankle Angle Profiles for Each Human Subject Test.....	84

Figure C.1.2	The Ankle Force Profiles for Each Human Subject Test.....	85
Figure C.1.3	The Ankle Torque Profiles for Each Human Subject Test	85
Figure C.1.4	The Torque-Angle Relationship for Each Human Subject Test	86

CHAPTER 1

Introduction

This thesis presents the design and validation of a novel ankle prosthesis. To better understand the novelty of the mechanism, some basic knowledge of normal human gait and existing prosthetic ankle designs are needed. Section 1.1 provides the motivation of the design of the prosthetic ankle. Section 1.2 introduces basic knowledge of normal gait analysis as a reference to evaluate the performance of the designed prosthesis. Section 1.3 presents an overview of current state-of-art prostheses and compares their technical specifications. Section 1.4 presents the objectives of the design and identifies the structure of the thesis.

1.1 Motivation

Ankle prostheses have long been an important alternative for below-knee (BK) amputees to regain the function of ambulation. Early ankle prostheses were just rudimentary devices used for foot replacement. They were worn more for a sense of “wholeness” of the human body than the physical functions [1]. Absence of normal human ankle functions results in uncomfortable walking, abnormal gait, and more energy expenditure.

Due to the large number of amputations during World War II, the U.S. government decided to fund researches in prostheses for veterans. Many novel and efficient prostheses were invented. Refinements in mechanisms and materials were made for lighter and more functional prostheses. Rather than simply provide basic limb appearance, these prostheses were designed to better return the full functionality of the lost body part to amputees.

In 2005, there were 1.6 million amputees living in the United States [2]. While cancer-related and trauma-related amputations are decreasing, amputations due to

vascular problems have increased dramatically over the past 20 years. Transtibial amputation (also known as below-knee amputation) accounted for 24.5% of all amputations [3]. Transtibial prostheses are designed to return amputees to a high functional level of ambulation. A natural foot is capable of storing energy during stance and returning it to the amputee to assist in propelling the body forward at push-off. The ankle joint produces most of the work. Together with the muscles along the leg, a natural human ankle provides the functions of shock absorption, motion control and power generation. However, both the ankle joint and the muscle complex are removed in a typical transtibial amputation. The challenge of the ankle prosthesis design is to find means to achieve the functions of an intact ankle, especially the function of power generation. Comfort and mobility are identified as the two primary benefits associated with an ankle prosthesis.

Current prosthetic designs provide a wide range of choices for below-knee amputees. The appropriate choice of prosthesis can significantly improve the comfort and performance of the patient. Most of the currently available prosthetic ankles, however, do not provide enough energy to propel the body forward. The primary motivation for this research is to design an ankle prosthesis that provides adequate ankle torque to propel the body forward during push-off.

1.2 Normal Gait

Human walking can be defined as a repetitious sequence of limb motions to provide the body both support and propulsion. It is necessary to understand normal gait before analyzing pathological gait. However, the terminology used to describe human gait varies considerably from one publication to another. The terms introduced by Dr. M. Whittle are used below [4]. The introduction in this section will first cover the fundamentals of normal gait and then the dynamic properties.

1.2.1 Fundamental Analysis of Gait

A single sequence of an individual limb motions resulting in the forward movement of the body is called a gait cycle (GC). Different phases are defined according to the position and kinematic relationships of the limb while walking. Figure 1.1 identifies the relationships among different terms used in describing a gait cycle. Because limb movements are continuous, it is hard to specify the starting or ending point of a cycle. The moment of floor contact is typically selected as the start of a gait cycle. It is generally called “initial contact” or “heel strike” (in some pathological gaits, patients do not contact the floor with their heel).

<i>Normal Gait Cycle</i>								
<i>Periods</i>	<i>Stance</i>					<i>Swing</i>		
<i>Phases</i>	Initial Contact	Loading Response	Mid-Stance	Terminal Stance	Pre-Swing	Initial Swing	Mid-Swing	Terminal Swing
<i>Tasks</i>	Weight Acceptance		Single Limb Support		Limb Advancement			

Figure 1.1 Functional Division of a Gait Cycle for a Single Limb

Each gait cycle can be divided into 2 periods: stance and swing. The duration of a complete gait cycle is known as the cycle time. The normal distribution is approximately 60% for the stance phase and 40% for the swing phase. The gait cycle can be further divided into 8 phases. The periods are divided by foot contact with the ground, and each phase is determined by the function of one limb. The progressive combination of phases enables the limb to accomplish 3 basic tasks: 1) weight acceptance; 2) single limb support; and 3) limb advancement. A detailed description of each task is presented below.

Weight Acceptance

Weight acceptance (WA) is the first task of the stance period. It starts with heel strike and ends with opposite limb swing; it involves the initial contact phase and the

loading response phase. Three functional demands (shock absorption, initial limb stability and preservation of progression) must be satisfied to accomplish the weight acceptance task. The challenge is to absorb the abrupt body weight transfer within a short time and to keep the balance of the body in a smooth sequence of motions.

Single Limb Support

Single limb support (SLS) begins with the opposite limb swing and continues until heel strike of the opposite foot. The stance limb is totally responsible for the task. Mid-stance phase and terminal stance phase are involved in SLS. The swing limb progresses over the stance limb, preparing for the next heel strike. Ankle angle changes from plantarflexion to dorsiflexion, and at the beginning of terminal stance, the heel rises and the body weight moves ahead of the forefoot for preparation of pre-swing.

Limb Advancement

Four gait phases are involved in limb advancement: pre-swing, initial swing, mid-swing and terminal swing. The largest amount of ankle torque and energy are generated during this task.

To meet the high requirements of limb advancement, the preparation starts at pre-swing phase within the stance period. The largest power burst occurs at the ankle during this phase. It starts with the initial contact of the opposite limb, then an abrupt transfer of body weight; a rapid unloading of the stance limb causing a forward “push” for the stance limb. This action is commonly called push-off.

Three swing phases follow the pre-swing phase and advance to complete the GC and prepare for the next stance phase. They are differentiated mainly by the positions of limb progression. Initial swing phase starts when the foot is lifted from the floor and ends when the swing limb is adjacent to the opposite limb. In mid-swing phase, the limb continues to advance until progressing over the stance limb and the tibia is vertical. Terminal swing phase finishes the advancement of the limb and prepares the limb for stance.

A single gait cycle is completed by accomplishing all the limb phases stated above. Repetitions of those phases continue to achieve the locomotion of the human body. Muscles together with ligaments and tendons help achieve the functions of human joints.

1.2.2 Dynamic Analysis of Gait

Dynamic analysis of human walking is an important aspect of gait research. It includes the displacements, forces, moments and energies of the system. Average ankle behaviors are presented in Figure 1.2 and Figure 1.3. They were obtained from a large number of natural human gait analyses by Dr. David A. Winter [5]. Figure 1.2 presents the average ankle force, torque and angle profile; while Figure 1.3 shows the typical torque-angle relationship that occurs during normal gait. The presented parameters were all measured in the plane of progression, which closely corresponds to the sagittal plane of the body in normal walking. The ankle angle is defined positive in dorsiflexion and negative in plantarflexion.

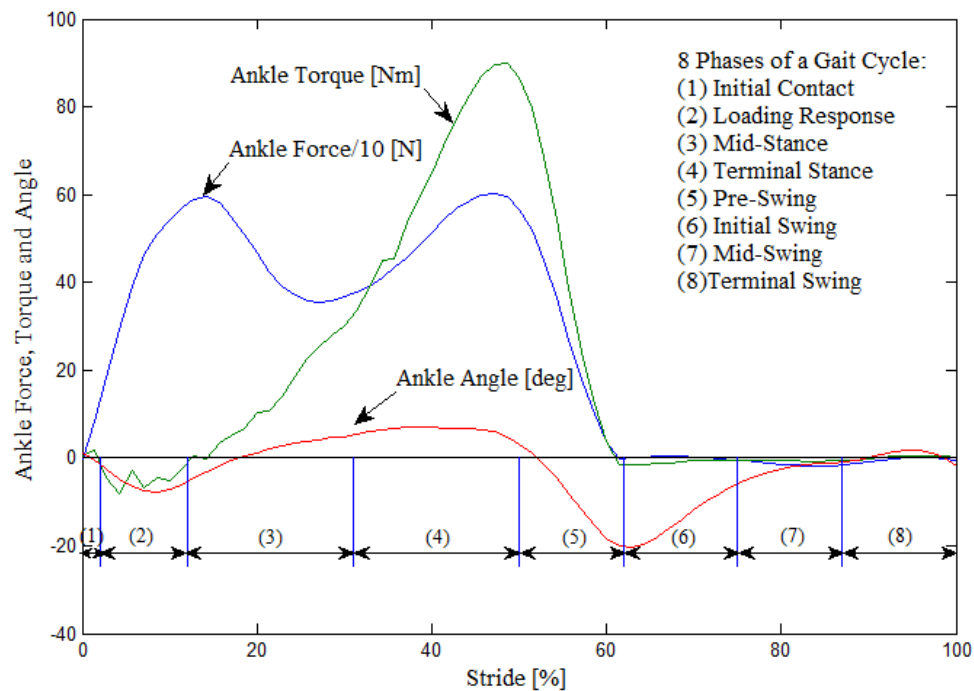


Figure 1.2 Ankle Force, Torque and Angle Profiles from Dr. Winter [5]

According to Winter's data, the deflection range of the ankle joint is approximately 27° . The ankle starts from a neutral position at heel strike and then goes to negative (plantarflexion) angle so that the forefoot is lowered to contact the ground. During the mid-stance phase and terminal stance phase, the ankle joint angle becomes positive (dorsiflexion). Then a large negative angle is developed during pre-swing phase. The ankle joint is moved back to neutral position during the swing period to prepare for the next gait cycle.

The ankle force profile presented in Figure 1.2 is the force along the leg axis. The ankle force has two distinct peaks. The first peak is caused by the impact of the foot during the loading response phase. The second peak occurs in the terminal stance phase, when the body prepares to move forward. The torque profile of the ankle has a small negative torque followed by a substantial positive torque. While the body continues to move forward, a large positive torque is created to propel the body forward [6].

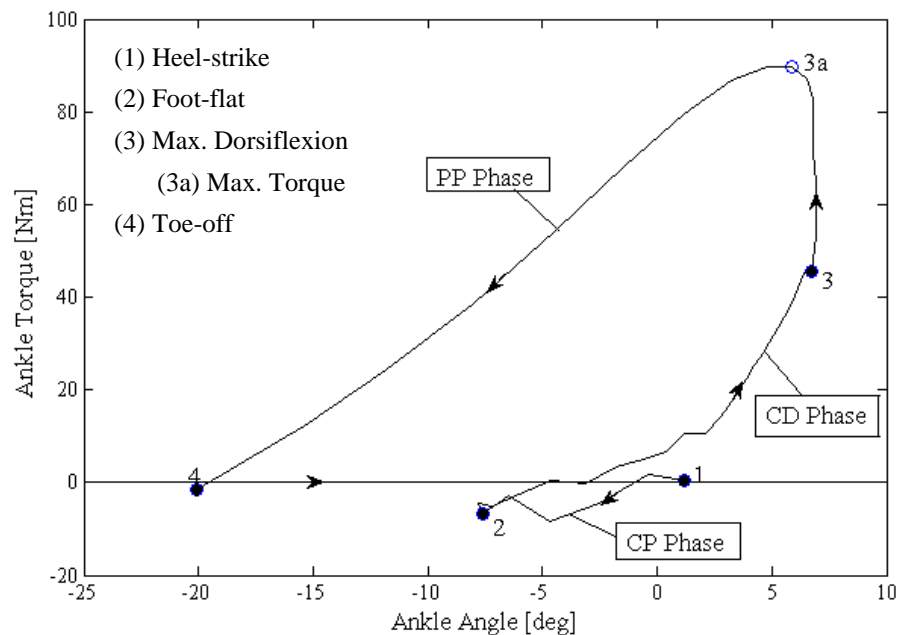


Figure 1.3 Torque-Angle Relationship from Dr. Winter [5]

In dynamic analysis, three distinct phases are often used to describe the torque-angle relationship in the stance period: Controlled Plantarflexion (CP), Controlled Dorsiflexion

(CD) and Powered Plantarflexion (PP) [7]. The instantaneous slope of the torque-angle curve indicates the instantaneous ankle stiffness. These three phases are each characterized by the instantaneous stiffness observed during the phase.

The CP phase, between time 1 and 2 in Figure 1.3, corresponds to initial contact phase and load response phase. During this phase, the foot initially contacts the ground and a nearly linear stiffness relationship is observed.

The CD phase is the interval from 2 to 3 in the figure. It corresponds to mid-stance phase and terminal stance phase. A nonlinear stiffness relationship occurs during this phase, and it shows that the ankle stiffness significantly increases with an increasing ankle angle.

The interval between 3 and 4 is described as the PP phase. From 3 to 3a, the ankle first achieved the maximum ankle angle at 3, and then the maximum ankle torque at 3a. This means that the ankle torque increases while the ankle angle decreases, which shows that additional energy is needed during PP phase to accomplish ambulation. Between 3a and 4, the ankle torque decreases linearly with decreasing ankle angle.

The ankle stiffness changes from positive to negative at 3. The sign change of ankle stiffness relates to the active ankle behavior. A large amount of torque used to propel the body forward needs to be generated while the ankle angle is decreasing. The amount of energy generated corresponds to the area between curves in torque-deflection profile in Figure 1.3.

1.3 Existing Ankle Prostheses

Two different approaches (passive and active) have been used to design ankle prostheses. Passive prostheses have been used for a long time. They are less costly and easier to use. Active prostheses, which have had a rapid development over the past two decades, provide energy to propel the body forward.

This section provides an overview of the technical approaches and performance of several existing state-of-the-art ankle prosthesis designs. The overview emphasizes their mechanical properties and their ability to enable the amputees to regain normal gait functions. An overview of popular passive ankle prostheses is presented first. The second part reviews several powered transtibial prostheses and compares their performance with a natural human ankle and with conventional passive prostheses.

1.3.1 Passive Prostheses

Most commercially available prostheses are passive devices. These devices use passive components such as springs and dampers in various forms. In general, there are two passive design types: the conventional Solid Ankle-Cushioned Heel (SACH) Foot and the Energy Storage and Return (ESAR) Foot. This sub-section describes these two passive prosthetic types and analyzes their strengths and weaknesses.

SACH Foot

The SACH foot is the most common prosthetic design and an excellent choice for amputees with an expected low-activity level. It is simple, durable and comfortable. The SACH foot is usually made of wood and rubber. As shown in Figure 1.4, the prosthesis mainly consists of a wood keel, a cushion heel, belting and plastic covering. It usually uses a bolt to attach to the pyramid or leg pylon. The wood keel is designed to provide base stability and rigidity. The cushioned rubber heel absorbs shock at impact and the belting allows for bending of the foot to mimic human ankle deflection. The density of the heel is an important design property. Belting is usually made of metal or plastic and it determines the resistance of dorsiflexion by its length extended from the ankle. The plastic covering protects the keel from the environment and gives the prosthesis an appearance very similar to a human foot.

SACH foot simulates plantarflexion at heel strike by the compression of the cushioned heel and provides dorsiflexion by the flexible belting. The SACH foot has a

very simple construction with no moving parts, which makes it easy to replace and maintain. Its light weight and low cost also make it an ideal choice for the basic ambulation need. The SACH foot provides choices for different sizes and heel heights. The SACH foot emulates the appearance of the human ankle well, but does less well in other functions. It provides no lateral movement, limited shock attenuation and very limited energy storage and release. Users typically are restricted to indoor walking or very limited outdoor activity.

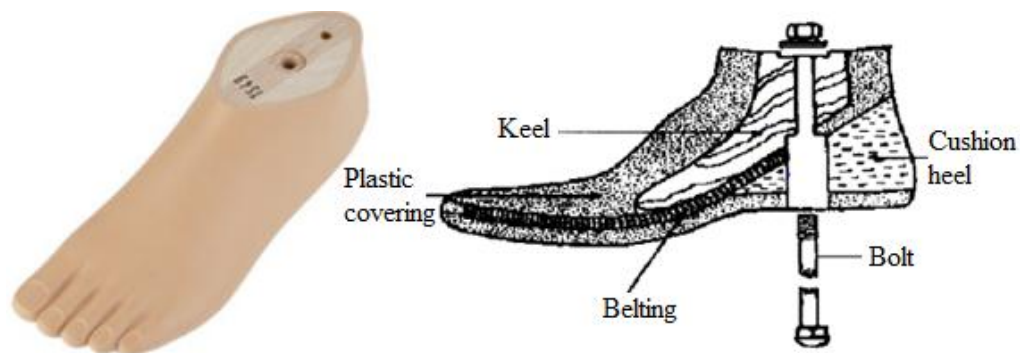


Figure 1.4 Models of SACH Foot

ESAR Foot

Since the first energy storage and return (ESAR) foot, the Seattle Foot, was introduced in 1981, many newer and more sophisticated designs have been developed to improve the performance of an ankle prosthesis. These prostheses are designed to store energy in early stance and return it to the amputee to propel the body in late stance.

An early ESAR foot looks very similar to a SACH foot. It usually incorporates a flexible keel and foam or rubber shell (Figure 1.5). It is the flexible keel that acts as an elastic spring, absorbing and releasing energy during push off.

New materials, such as carbon composites, have become available for prostheses as technology has advanced. A totally different type of ESAR foot, the Flex Foot, is now the most common prosthesis. It typically contains a flexible carbon fiber shank and a heel spring. Except for the ankle and foot portion, the Flex Foot extends the length of

prostheses and allows the entire device to flex, to absorb and return energy [8]. Different functions are provided with various designs. All models offer significant advantages over conventional SACH prosthetic feet. The heel spring in the Flex Foot system acts like a compressible foam with a great ability of energy storage and return. It is compressed and stores energy in early stance and slowly releases the stored energy as the foot moves forward. As the heel stiffness increases, the duration of shock absorption decreases and less energy is wasted. Some latest designs of Flex Foot add additional springs or dampers along the shank, which allows multi-axis movement and superb shock absorption. A more comfortable and responsive feel to the user is provided with this design.



Figure 1.5 ESAR Feet
(Upper: Seattle Feet from Trulife; Bottom: Flex Feet form Óssur)

Although current passive prostheses try to mimic the energy storage and return observed in human ankles, none of the commercially available prostheses can provide adequate energy needed for forward propulsion during push off. Below-knee amputees

with prosthetic devices still need to expend 20% — 30% more energy than people with natural ankles to walk at the same speed [9]. Powered prostheses, which use active components such as motors and actuators, are being developed to address this problem.

1.3.2 Powered Prostheses

Studies reveal that the human ankle absorbs energy and produces more energy than it absorbs [10]. For an artificial foot, the additional energy can be obtained from some other source. The use of improved motor technologies allows active alternatives to passive prosthesis design. Except for weight and cosmetic appearance, powered prostheses are better at emulating the functions of human ankle joint. Several active approaches are described below.

SPARKy

The SPARKy prosthesis, short for Spring Ankle with Regenerative Kinetics, is an active prosthesis to apply regenerative kinetics to its design. It was designed by Dr. Thomas Sugar and his group from Arizona State University. The design emphasis was to bring full human ankle functions to transtibial amputees, particularly those who wish to return to active duty in the military [11]. It is designed to provide enhanced ankle motion and push-off power comparable to that of an able-bodied person. Three iterations of the SPARKy prosthesis have been issued, with each one providing a more compact and efficient prosthesis. The latest issue (SPARKy 3) has two degrees of freedom with reduced size and weight compared with other two. Human subject tests of the devices proved its capability of reproducing the motion and the power of a healthy ankle [12].

The main structure of SPARKy 3 (Figure 1.6) contains two motors, a flex foot, two helical springs, a robotic tendon actuator (L-arms driven by ball screws to transfer the linear actuation to the helical springs), rotational joints and a pylon. SPARKy 3 operates by actively engaging the helical springs to store energy while the leg rolls over the ankle and uses the robotic tendon actuator to add the energy needed to propel the body forward.

The robotic tendon actuator features small motors in series with helical springs. Because of the helical springs, the energy requirements on the motor are reduced. Instead of a gearbox, ball screws are used as transmissions here to efficiently reduce the overall size and weight. The L-arms act like levers to further decrease the size of the actuator and relieve part of the load on the ball screws.

A two DoF joint is designed around the rotational center of human ankle. The coronal ankle axis and the primary ankle axis are orthogonal and connected with a customized U-joint (a combination of two socket arms shown in Figure 1.6). To increase the ankle stability and better emulate human ankle deflection, custom limited-motion bearings are used to add angular stiffness about the coronal axis.

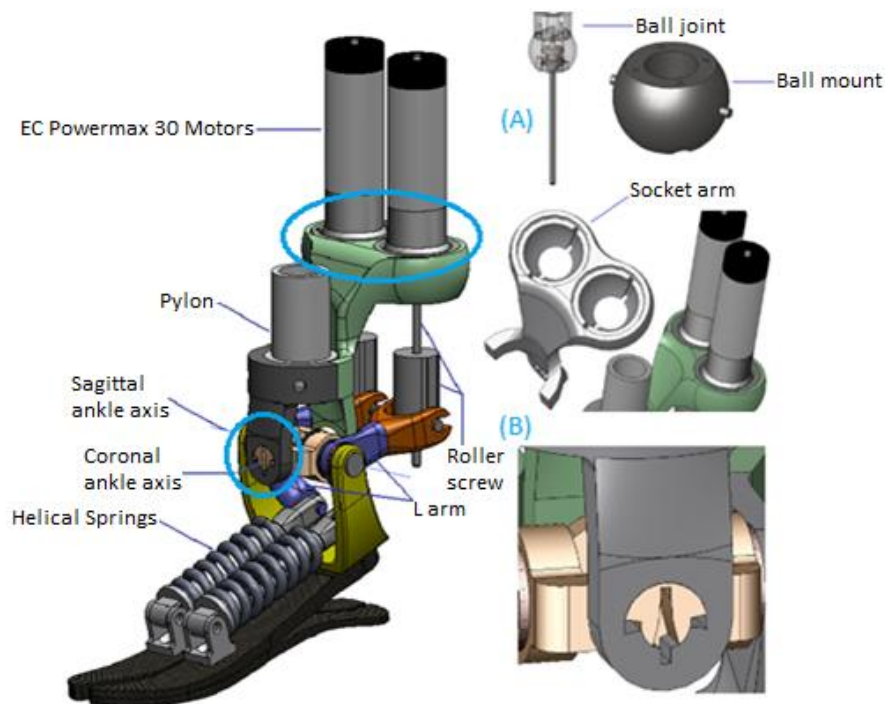


Figure 1.6 CAD Model of SPARKy 3
(A: Ball Screws and Socket Arms; B: Custom Bearing Design) [12]

SPARKy 3 uses basic components to make an active device. The two motors, coupling with the energy achieved from the helical springs, are capable of producing up to 200 *Nm* of peak moment. It provides functionality with enhanced ankle motion and

power. SPARKy 3 also allows users to walk on different terrains as well as stairs and slopes. The control system for SPARKy is based on various patterns of normal gaits. The locations of ankle joints and springs are predetermined and adjusted for maximum efficiency. However, this technology is not fully developed and complex phase-plane movement can hardly be achieved. Another limitation of this design is the high battery capacity requirement due to the use of two motors [13].

PowerFoot One by iWALK

iWalk's PowerFoot One (Figure 1.7) is the world's first commercial powered ankle prosthetic. It is initially designed and built at the MIT Media Lab led by Dr. Hugh Herr. It is designed to generate human-like power at the ankle joint with both passive and active components. It also can adjust to stairs and slopes ascending and descending. The PowerFoot One, equipped with three internal microprocessors and twelve sensors to measure forces and positions, can be adjusted using a remote controller [14]. The measurements are compared with comprehensive human movement patterns and the microprocessors decide the way the prosthesis will operate. Both the physical positions and the mechanical behaviors of the ankle are considered in the design.



Figure 1.7 Original PowerFoot One by iWALK Company [14]

The modification of PowerFoot One is shown in Figure 1.8. It mainly consists of five parts: a brushless DC motor, a ball-screw transmission, a unidirectional parallel spring, an in-series leaf spring and a carbon composite foot. The motor, the transmission and the in-series leaf spring are combined to form a force-control actuator called Series-Elastic Actuator (SEA). The SEA is used to control the position of the spring, modulate the ankle stiffness and provide adequate ankle torque [15]. The rotary motion of the motor is transformed into linear motion through the ball-screw transmission. The leaf spring stores and releases energy delivered by the motor. Sensors are used to detect the deflection of the spring for the controller to decide the force to apply. A unidirectional leaf spring engages and stores energy when the prosthetic ankle angle is less than 90° and becomes unengaged at angles greater than 90° . This is used to mimic the nonlinear behavior of the human ankle. The carbon composite foot provides additional compliance in the heel and forefoot. A Lithium-Polymer rechargeable battery is used to provide energy to the motor and has been housed together with the motor and other electronics within the top part of the prosthesis.

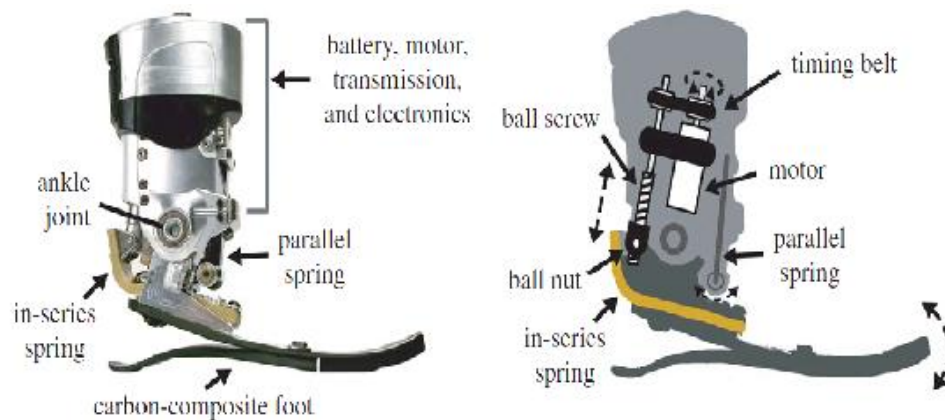


Figure 1.8 PowerFoot One model [15]

This powered prosthesis is found to reduce the metabolic cost for all participants, compared to the conventional passive-elastic prostheses (Flex Foot). The result supports the hypothesis that a powered ankle-foot prosthesis can improve amputee walking

economy. Although the PowerFoot One is called the most advanced prosthesis currently developed, the cost for the prosthesis is quite high (about \$76,000).

Active Four-Bar Prosthesis in Parallel with a Torsional Spring

A powered prosthesis with four-bar mechanism was designed and built by Dr. Phillip Voglewede and his students at Marquette University. The prosthesis is designed to achieve a greater range of ankle motion and enable amputees to return to a more normal ambulation level with minimal energy input. The critical part of the design is the use of a four-bar mechanism in combination with a torsional spring to achieve the nonlinear stiffness behavior of a human ankle. Figure 1.9 presents a not-to-scale conceptual model of the four-bar prosthesis. The relative lengths of the four connected bars and ankle joint stiffness were optimized to achieve the design objectives of energy efficiency and compactness.

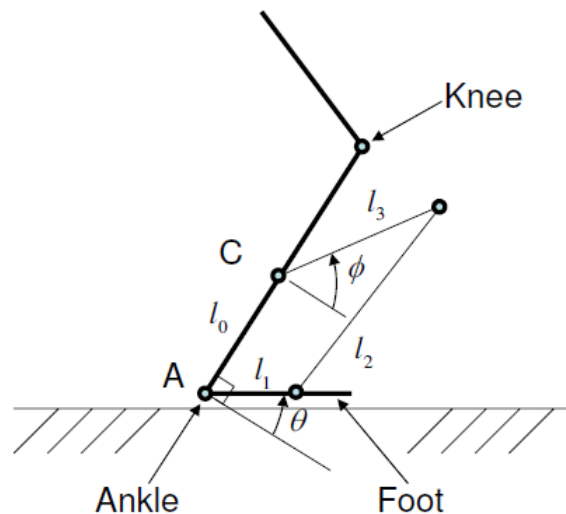


Figure 1.9 Model of the four-bar prosthesis configuration. [16]

The four-bar prosthesis mainly consists of a brushed DC motor, a transmission, a four bar mechanism, a torsional spring and an aluminum foot. Figure 1.10 shows the proof-of-concept prototype prosthesis. The four-bar mechanism combined with the torsional spring and motor are used to achieve the active and nonlinear behavior of a natural human ankle. The mechanism converts the linear spring stiffness at one joint (C

in Figure 1.9) into nonlinear spring stiffness at the ankle joint (A in Figure 1.9). The DC motor provides the extra torque needed during push off. A 50:1 gearhead is used as a transmission. Although the weight is sacrificed in this design, the requirements for motor power and battery capacity are both reduced.

Human subject tests have been successfully conducted with this prosthesis design. Results showed that the prosthesis did provide more ankle moment and did match Winter's torque profile much better than a passive prosthesis. However, this design is less compact than desired. The control system and battery for the prosthesis are mounted on a relatively bulky backpack, which partly restricts the ambulation of the subject [16].

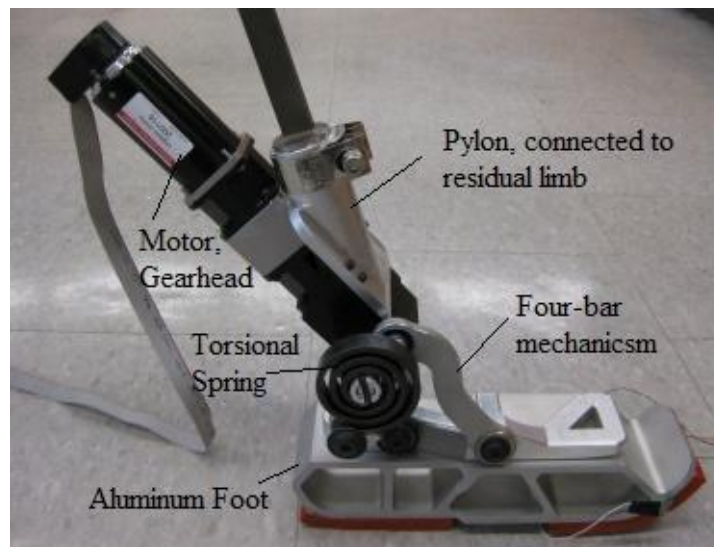


Figure 1.10 The Prototype of the Four-Bar Prosthesis [16]

CESR Prosthesis with Microprocessor

A new prosthetic foot technology designed to reduce the metabolic energy demand of an amputee was developed by Dr. Authur Kuo and his students at the University of Michigan. The Controlled Energy Storage and Release (CESR) foot uses a microprocessor-controlled spring mechanism to store elastic energy during heel strike and release that energy at the optimal timing. Figure 1.11 presents the prototype model of the CESR foot and describes the energy recycling sequence during walking.

The energy-recycling prosthesis is comprised of six components: the attachment interface, the toe assembly (forefoot), the heel assembly (rear foot), the primary compression spring, the heel clutch, and the toe clutch. The heel clutch, together with the mid-foot joint, allows the heel to rotate freely in plantarflexion to compress the spring and locks when the force is in the opposite direction. The toe latch prevents the forefoot from rotating about mid-foot axis in plantarflexion unless unlatched. Heel and toe clutches could both be released by the micro-motor actuator. The microcontroller is used to adjust the timing of energy release (unlatching the toe clutch). It delays the return of energy until push-off, where it acts as a partial substitute for the intact ankle.

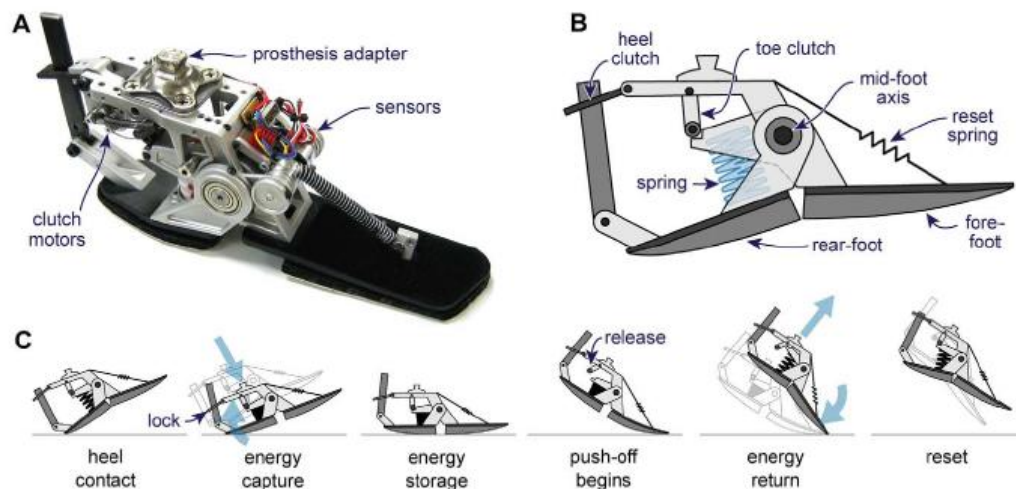


Figure 1.11 CESR Prosthesis [17]

(A: Model of the device. B: Schematic design. C: The energy recycling sequence)

The CESR mechanism is a “semi-active” energy-recycling artificial foot. All the energy activities are performed by passive components; only a microcontroller and two micro-motors are used as active elements to release the clutches and reset the mechanism. No additional ankle torque is provided by the motors to help propel the body forward. The device can be powered by a small battery at only 0.8 W. Tests have been conducted upon healthy subjects by wearing a simulator boot to immobilize the test ankle and a lift shoe on the healthy foot. Test results show that subject wearing conventional prosthesis

spend 23% more net metabolic energy expenditure, but have only 55% ankle push-off energy compared to normal walking. CESR foot restored ankle push-off energy to 7% above normal level and reduced the net metabolic energy expenditure by 9% compared to conventional prosthesis. Although this prosthesis design still spends 14% more metabolic energy than normal ankle, it has been shown to reduce the metabolic energy of ambulating by 40% (compared to conventional prosthesis). Increasing the capability of energy storage and precision of energy release timing will contribute to further reduce the energy expenditure of the prosthesis [17].

1.3.3 Summary

In comparing passive and active prostheses, several criteria should be considered. They are:

- (1) Portability: A key concern for prostheses is portability. Size and weight are important design criteria. Thus active devices that require large actuators and batteries may limit portability.
- (2) Cost: Although high-tech inventions often achieve good results, they do cost much more money. The inventions with the biggest impact are often the ones that remain simple and affordable.
- (3) Power Supply: Active prostheses use power supplies to help the amputee walk easier. Size, weight, and recharge frequency of the supply must be considered in the design.
- (4) Energy Efficiency: A good prosthesis design is one whose energy use is efficient. Designs that use both active and passive components can often provide a more efficient solution [18].

Since a passive device does not have an actuator or power supply, only criteria 1 and 2 are considered. Criteria 3 and 4 are mainly aimed at active devices. All the

active prostheses discussed in Section 1.3.2 used passive components (series elastic actuator or springs) to help achieve better performance.

1.4 Goal of this Research

The goal of this research is to design a passive prosthetic ankle that looks and behaves more like a normal ankle. With high performance passive components, the prosthesis could store elastic energy during heel strike and return it to the amputee to propel their body forward during push-off.

This thesis primarily focuses on the mechanical design and testing of a novel passive ankle prosthesis. The prosthesis structure and components were designed and chosen to achieve the design criteria listed in Section 1.3.3 with particular emphasis on the characteristics of lightweight, low friction and compactness.

Chapter 2 provides a review of the conceptual model of the prosthesis functions that are the basis of this work. Chapter 3 details the design processes and presents the reasons why particular dimensions and components were chosen for use. Chapter 4 presents the pre-test preparations and discusses the results of robot tests and human subject tests. In Chapter 5, the conclusions and future work are provided.

CHAPTER 2

Conceptual Design

As stated previously, this thesis describes the design and testing of a novel ankle prosthesis. The novel prosthetic ankle is based on a previously developed ankle prosthesis concept that uses coupled compliances to increase ankle torque [19]. A network of springs is used to store and release energy to provide active nonlinear behavior similar to that of a natural human ankle. An overview of the passive ankle design concepts and optimization are presented in this chapter.

Section 2.1 identifies the design criteria used to guide the development of the prosthetic ankle. Section 2.2 describes the conceptual model of the prosthesis as well as the strategy used to satisfy the design criteria. Section 2.3 describes the optimization procedures and results for the prosthesis designed to match the behaviors of a natural ankle.

2.1 Design Criteria

As stated previously, the design objective is to build a prosthetic ankle that looks and behaves more like a natural human ankle in aspects of appearance, weight and dynamic characteristics. This section explains the design criteria used to guide the prosthesis design.

This ankle prosthesis will use purely passive components to convert an adequate amount of energy to propel the body forward and achieve active behavior similar to that of a human ankle. The prosthetic ankle design criteria provided below relate to aspects of physical properties and mechanical performance. The design criteria are:

1. The prosthesis should be compact in construction;
2. The prosthesis should be light in weight;
3. The prosthesis should be quiet during its operation;

4. The prosthesis should return to its natural or equilibrium position to prepare for the next gait cycle during swing period (both ankle force and angle should return to zero);
5. The prosthesis should operate in a way similar to that of a human ankle;
6. The prosthesis should have a torque profile similar to that of a human ankle.

Prosthesis compactness ensures that it is suitable to use for various locations of transtibial amputations. An ideal design should fit within an unmodified shoe so that the exterior appearance is similar to that of a normal leg. As there is no external energy input, the amputee is expected to lift the leg after push-off. In order to aid in gait transitions and make a more comfortable walking experience, the prosthesis should be lightweight. This is one of the primary advantages of passive devices.

As a passive prosthesis, the design is focused on the device behaviors when it is in contact with the ground, i.e., the stance period of the gait cycle. During the swing period, the prosthesis moves together with the residual limb. In order to continue the repetitive sequence of limb motions, the prosthesis must return to its equilibrium position to prepare for the next gait cycle at the end of stance period, i.e., just after the mechanical push-off.

To improve the performance of a passive ankle prosthesis, a better match to human ankle behavior is desired. Mechanical behaviors of a normal ankle are characterized by parameters such as the ankle force along the leg axis, the torque about the ankle and the angular deflection of the ankle. When modeling and optimizing prosthesis mechanical behavior, the torque profile of the human ankle during walking is chosen as the parameter used for evaluation. The calculated torque profile of the prosthesis should match the natural torque profile as much as possible to demonstrate improved performance.

The criteria identified above are the primary design considerations. The strategies used to realize the prosthesis designs that satisfy these criteria are presented in the following section.

2.2 Design Strategies

The ankle prosthesis in this research is designed to store and return elastic energy to the amputee to propel body forward during push-off. As no motor or actuator is used, the passive ankle prosthesis must store enough energy in *ankle and leg deflections* for later release when used to propel in body forward. The criteria identified above must be simultaneously considered during the design process. Design strategies used to obtain the desired behaviors are presented in this section.

2.2.1 Use of Conventional Passive Springs

In this approach, the ankle prosthesis is a mechanism having 2 coupled DoF with a network of conventional compression springs. One DOF allows the amputee to slightly compress the lower leg when weight is applied; the other allows the foot to rotate about the ankle joint. By coupling the two DoF, the force generated along the leg can be transformed into ankle moment to more closely match human ankle behavior.

A network of springs is used to store and release energy in the prosthetic ankle. Springs provide an efficient way to store and release energy. They are also quiet, small and lightweight. A natural leg does not have perceptible deformation when walking; however, deflection along the leg is needed to store energy for propulsion. Stiff compression springs allow the prosthesis to store a large amount of energy with a small deflection along the leg axis. If the deflection is limited to less than a half inch, the prosthesis will perform in a way that is very similar to that of a natural ankle and provide a comfortable walking experience.

Spring rates and spring connecting locations are selected to match the natural ankle torque profile. During stance period, three tasks must be accomplished by the selected spring network.

2.2.2 Task 1: Obtain Nonlinear Stiffness

In Figure 1.3 (torque-angle relationship), nonlinear stiffness of the human ankle is observed through the slope changes of the curve. During the Controlled Dorsiflexion phase (from 2 to 3 in Figure 1.3), stiffness properties are nonlinear. To obtain this nonlinearity, a changing spring connection geometry resulting from the ankle deflection is used. The change in spring connection geometry and the stiffness nonlinearity are illustrated in Figure 2.1.

Deflection $\delta_{A/B}$ is the relative displacement between the two connection points, and δ_k is the spring deflection. Note that $\delta_{A/B}$ is not always along δ_k . When the ankle angle decreases (from Figure 2.1 a to 2.1 b), the angle between $\delta_{A/B}$ and δ_k decreases, which means that the relative motion between connection points more closely matches the spring axis. Thus the stiffness at the ankle joint is increased.

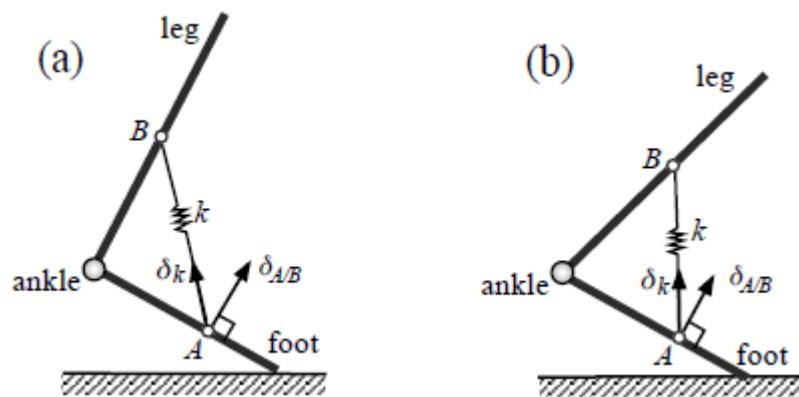


Figure 2.1 Stiffness Nonlinearity: Stiffness changes as ankle angle deflects

The torque-angle relationship shown in Figure 1.3 also shows different stiffness behaviors for deflection at different ankle deflections. The slopes observed from 1 to 2 are different from those going from 2 to 3. To achieve this type of nonlinearity, two different sets of springs are used and unilaterally connected at different sides of the leg. As shown in Figure 2.2, compression springs are used to provide unilateral compliance

for a specific range of ankle motion. One set of springs is engaged when $\theta > 0$; and a different set is engaged when $\theta < 0$.

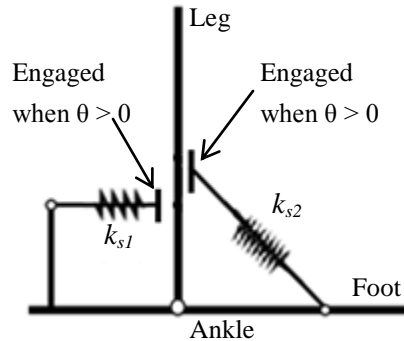


Figure 2.2 Two sets of Unilateral Compression Springs

2.2.3 Task 2: Generate Adequate Torque at the Ankle

Two sources of energy input can be used during the stance period. One source is the user's weight (static load), the other is dynamic load due to body acceleration. Usually, the dynamic load is around 20% of the user's weight [20]. A passive prosthesis should absorb energy from these loads and release it later at the push-off.

The torque generated by the deflection of the ankle in Task 1 is not nearly enough to provide adequate torque for push-off [4]. Additional ankle torque should be generated to help to propel body forward. It is important to notice that, in the early Powered Plantarflexion phase (from 3 to 3a in Figure 1.2), the force along the axis increases dramatically. This force can be transformed into torque about the ankle. An elastic mechanism, the spring k_2 together with slider shown in Figure 2.3, is used to couple the leg motion (deflection along the leg axis) with the angular ankle deflection (ankle angle). The top end of spring k_2 can move along the leg axis and the bottom end of spring k_2 is moved away from the rotation point (ankle joint). In this way, the spring k_2 can be compressed by the deflection along the leg axis and generate torque about the ankle. The off-leg-axis track is designed to guide the slider (one spring end) further away the

rotation point. Additional torque is generated when the leg is further loaded. Parameters of the spring connection locations are shown in Figure 2.3.

The energy stored in the passive prosthesis is related to the ankle deflection. If unregulated, the energy stored during dorsiflexion would be released during plantarflexion before push-off and therefore unavailable to generate the necessary torque. As stated previously, energy stored from ankle deflection motion is not enough for push-off; the energy stored in the k_2 spring system from leg deflection must also be retained. A lock mechanism is designed to hold the energy and prevent early release. This mechanism allows the stored energy to generate positive torque about the ankle even when the force along the leg is decreasing and the ankle deflection is in the opposite direction. A corresponding unlock mechanism is used to release the spring and ensure that the system returns to its equilibrium position at the end of the stance period.

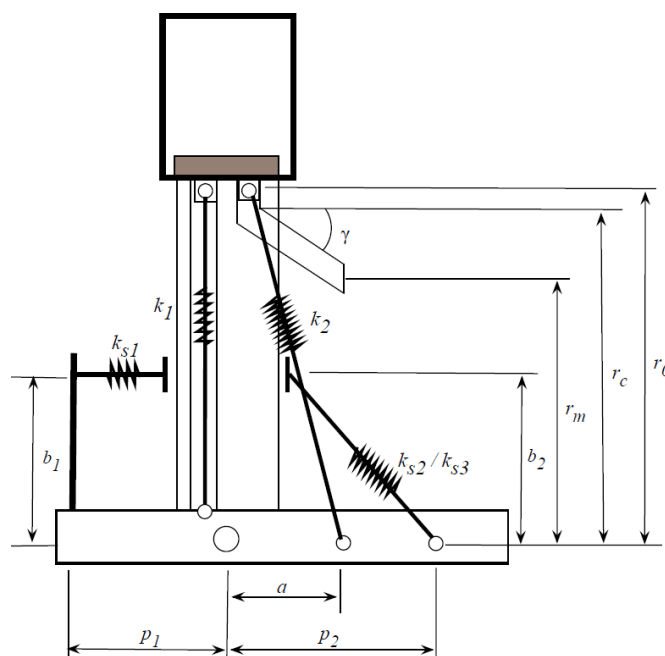


Figure 2.3 Spring Connection Geometry

A simple model of the prosthesis and its dimensions are shown in Figure 2.3. For the off-axis track, r_0 is the starting point of the track; r_c is the location where the track is directed off the leg axis; r_m is the bottom position of the track and γ is the angle of the

off-axis track. Angle γ and bottom location r_m determine the distance the spring connection moves away from the leg axis.

2.2.4 Task 3: Match the Natural Torque Profile

To better match the natural torque profile, two sets of springs are added to the system (as shown in Figure 2.2). These two sets of springs are called bottom springs and are only related to ankle deflection. As stated in Task 1, each set of bottom springs provide unilateral compliance with different ankle deflection.

Spring set k_{s2} / k_{s3} uses a similar spring connection method as spring k_{s1} . The tilted spring axis adds nonlinear stiffness to the system. To further match the peak value and the large torque in the early PP phase, two stiff springs with different free lengths are used (as shown in Figure 2.4). In this design, spring k_{s2} is engaged first and the spring k_{s3} is engaged after a certain amount of additional ankle deflection. Working together with the stored energy in spring k_2 , the ankle torque of the designed prosthesis is expected to reach a similar peak value as that of the human ankle.

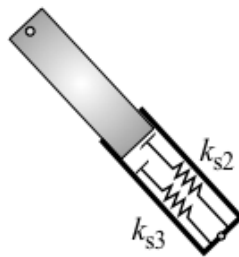


Figure 2.4 Design of Bottom Springs with Different Free Lengths

2.3 Conceptual Model of the Passive Ankle Prosthesis

From the simple model presented in the last section, a mechanical model is developed in this section. The definitions of moving parts and their relationships during operation are described as follows.

The ankle prosthesis consists of four primary bodies and the five sets of springs.

Figure 2.5 shows the structure of the conceptual ankle prosthesis.

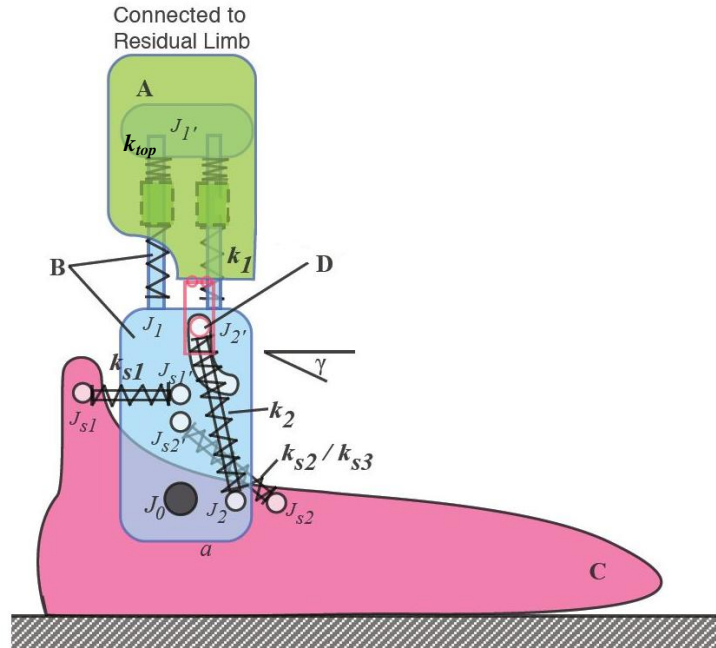


Figure 2.5 Embodied Mechanical Model of the Prosthetic Ankle

The bodies are:

- A upper-leg A, connecting the prosthesis to the residual limb;
- A lower-leg B, attaching to the upper-leg A with sliding joints, rotatable to the ankle joint;
- A foot C, the base of the prosthesis, attaching to the lower-leg B by a revolute joint, which represents the ankle joint in this design;
- A body D, moving along the track on the lower-leg B.

The springs are:

- Spring k_1 connects lower-leg B and upper-leg A respectively at J_1 and J_1' ;
- Spring k_2 connects foot C and body D at joint J_2 and joint J_2' ;
- Springs k_{s1} connects foot C and lower- leg B respectively with joints J_{s1} and J_{s1}' ;

4. Spring set ks_2/ks_3 connects foot C and lower leg B respectively with joints J_{s2} and J_{s2}' , the two spring sets share the joint and the spring axis but have different stiffness and free lengths.

In Figure 2.5, joint J_0 represents the position of human ankle joint. Joints J_0, J_2', J_{s1}' , and J_{s2}' are collinear along the leg axis. Springs ks_1 is engaged only when ankle rotates in plantarflexion direction. Spring set ks_2/ks_3 is engaged only when ankle rotates in dorsiflexion direction.

The movements of the prosthesis during the stance period are designed to ensure that the device can achieve the performance objectives. Figure 2.6 shows the relationships between bodies and spring mechanisms during operation. Descriptions for each step are presented below.

Figure 2.6 (1) illustrates the heel strike position of the prosthetic ankle. The back rounded part of foot C represents the heel of a human foot. When the heel contacts the ground, body weight is gradually transmitted to the prosthetic ankle. As a result, body D begins to slide along the track on lower-leg B. Spring k_1 is compressed by upper-leg A and generates the force along the leg; spring ks_1 and spring k_2 are engaged and generate the positive torque about the ankle joint J_0 . As walking continues, the whole foot will be in contact with the ground and the ankle deflection will change from plantarflexion to dorsiflexion.

Figure 2.6 (2) illustrates the foot flat position of the prosthetic ankle. As the deflection of ankle increases, spring set ks_1 returns to its free length and spring set ks_2/ks_3 are engaged successively. Spring sets k_1 and k_2 are further compressed. After fully loaded by body weight, the ankle reaches the maximum dorsiflexion angle, thus spring sets k_1, k_2, ks_2 and ks_3 are fully compressed. Body D is held at the bottom position of the off-axis track by the lock mechanism, thus the energy stored in spring k_2 is not released immediately.

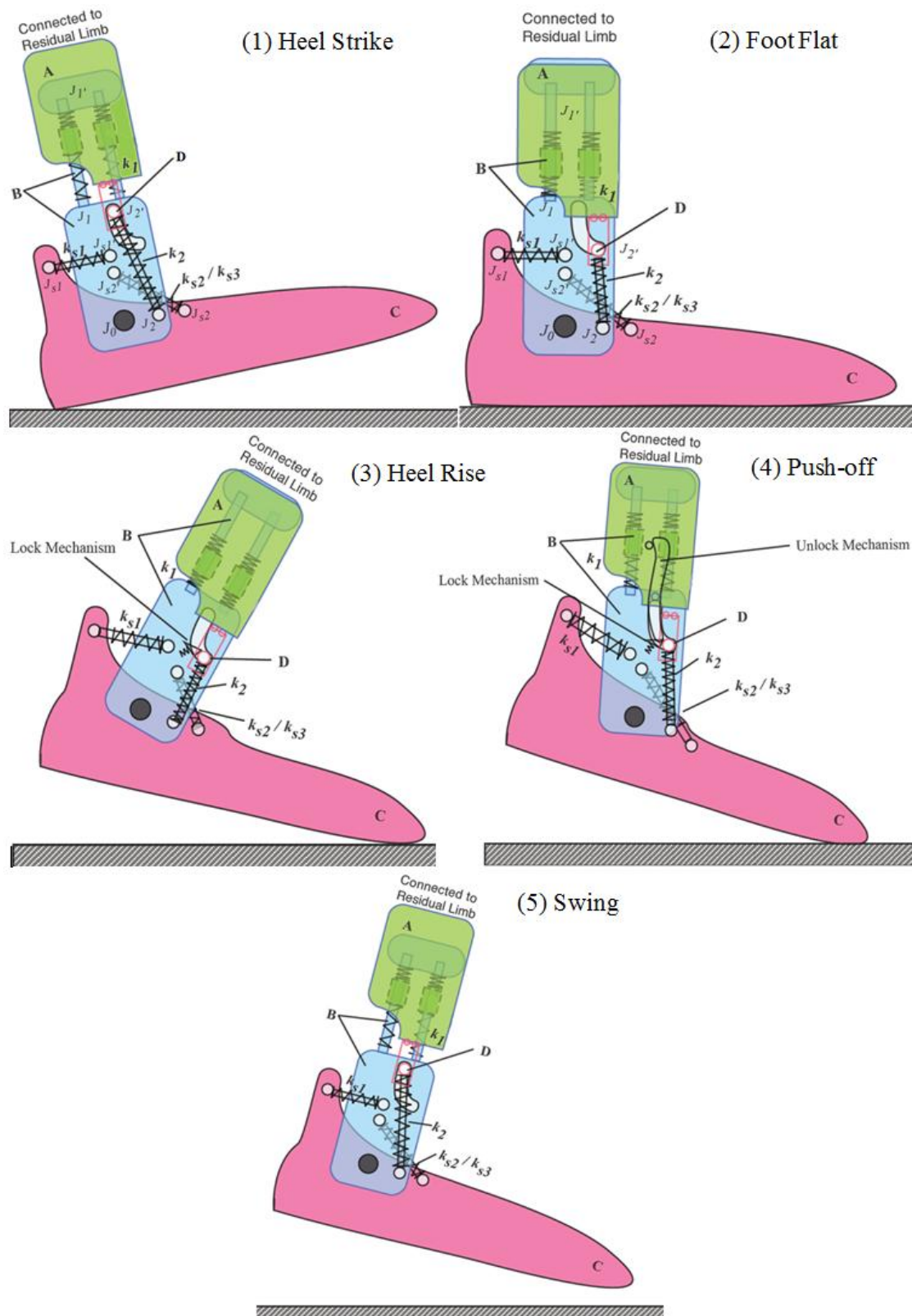


Figure 2.6 Movements of Prosthetic Ankle during Stance Period

Figure 2.6 (3) shows the heel rise position of the prosthetic ankle as well as the position of the lock mechanism. From heel rise to toe-off, the dorsiflexion angle decreases and changes to plantarflexion and the upper-leg A moves upwards. Thus spring sets k_1 , ks_2 and ks_3 are gradually released back to their original length while spring set k_2 still stays compressed to generate sufficient torque about the ankle for push-off.

Figure 2.6 (4) shows a push-off position of the prosthetic ankle and the unlock mechanism. When upper-leg A and spring set k_1 return to their original position, the unlock mechanism is triggered to release the spring set k_2 so that the ankle can return to its unloaded position.

Figure 2.6 (5) illustrates the swing position of the prosthetic ankle. All the mechanisms and springs have returned to their original position and ready for the next gait cycle.

2.4 Optimization Process and Results

The analyses presented above shows that the designed prosthesis can mimic the walking pattern of human ankle. An optimization was conducted using MATLAB to make an optimal mechanical design and obtain the best match of natural ankle behaviors.

When modeling and analyzing the mechanical behavior, it is important to consider system inputs and system outputs. A vector of design variables $\mathbf{X} = [k_1, k_2, ks_1, ks_2, ks_3, r_0, a, \gamma, b_1, b_2, p_1, p_2]$ is used in the optimization. The spring ks_3 is engaged when ankle angle is 6.8° in dorsiflexion direction. The free length of spring ks_3 is calculated and represented as Ls_3 . The variables are optimized in the program and yield a calculated torque profile $\mathbf{T}(t)$ that best matches that of a human ankle.

In order to get the output, four inputs are provided. The program inputs are the deflection of the ankle $\theta(t)$, force along the leg $\mathbf{F}(t)$ and the natural ankle torque profile $\mathbf{T}^N(t)$. An initial set of design parameters \mathbf{X}_0 is given to start the optimization. All functions $\theta(t)$, $\mathbf{F}(t)$ and $\mathbf{T}^N(t)$ are obtained from experimentally observed normal human

gait analyses [5]. The natural ankle torque profile $\mathbf{T}^N(\mathbf{t})$ is given as a target for the optimized output $\mathbf{T}(\mathbf{t})$ to match. The deflection along the leg is calculated as Δr .

To match the natural ankle torque, the deviation between the calculated torque and the natural torque is minimized. The optimization is formulated as:

$$\begin{aligned} \text{Minimize:} \quad & f = \mathbf{T}(\mathbf{t}) \mathbf{T}^N(\mathbf{t})^2 \\ \text{subject to:} \quad & \mathbf{X}_{lb} \leq \mathbf{X}_0 \leq \mathbf{X}_{ub} \\ & \max(\Delta r) \leq 0.013 \text{ (m)} \end{aligned}$$

where \mathbf{X}_{lb} is a vector of lower bound values and \mathbf{X}_{ub} is a vector of upper bound values.

The mechanical parameters is generated from the input $[\boldsymbol{\theta}(\mathbf{t}), \mathbf{F}(\mathbf{t}), \mathbf{T}^N(\mathbf{t})]$ and the initial set \mathbf{X}_0 . Many optimizations were performed, each with a different initial set of \mathbf{X}_0 . For compactness, the values of b_1 and b_2 are set to be the same. In this initial optimization, the optimized prosthetic torque profile (no presented) calculated from this set of parameter values closely matches the natural ankle torque. The prosthetic torque has the same peak value as the natural ankle torque and the interval between the two torque peaks is only 3.5% of the stride.

However, after the design and fabrication of the prosthesis, tests showed that the displacement of the prosthesis along the leg was much less than expected for the device. The program used to calculate the force-deflection relationship was further evaluated. An error in picking the angle between spring k_2 and the inclined track in the MATLAB inverse sine function was found. With the same function value, MATLAB always picks the smaller angle, which was inappropriate in this situation. This mistake resulted in obtaining an oppositely directed force in the MATLAB calculation from the correct value. This caused the optimization to select inappropriately large spring rates. After revising the program, a new optimization was performed. Since the device was already fabricated, all the geometry dimensions were unaltered to avoid constructing a new device. The spring rates were modified according to the new optimization. All design parameters values obtained in the second optimization are presented in Table 2.1.

The prosthetic ankle torque profile of the second optimization is compared with the natural ankle torque profile in Figure 2.7. The optimized prosthetic ankle has a typical single-peak torque profile. However, the ankle torque curve of the prosthesis does not closely match the natural ankle torque. The ankle prosthesis reaches its peak value earlier than a natural ankle. In addition, the peak value of the prosthesis torque is 0.84 Nm/kg , which is only 53% of natural ankle peak torque.

Table 2.1 Optimized Mechanical Parameters

Parameters	Values	Parameters	Values
k_1	18 (N/mm)	b_1	0.06 (m)
k_2	45 (N/mm)	b_2	0.06 (m)
ks_1	10 (N/mm)	p_1	0.057 (m)
ks_2	140 (N/mm)	p_2	0.06 (m)
ks_3	30 (N/mm)	Ls_3	0.073 (m)
r_0	0.098 (m)	r_c	0.096 (m)
a	0.026 (m)	r_m	0.086 (m)
γ	35.29 (°)		

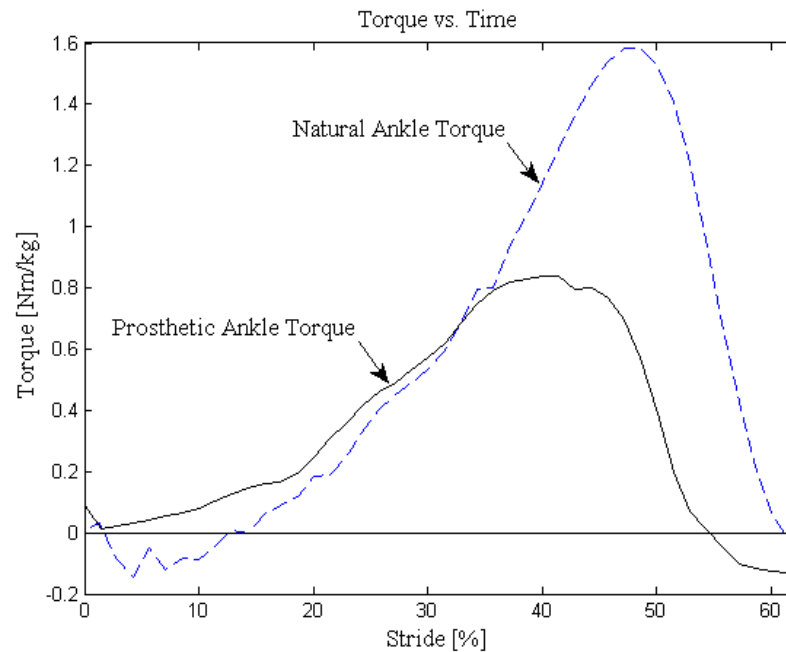


Figure 2.7 Torque Profile of the Prosthetic Ankle from Optimization

Figure 2.8 shows the torque-angle relationships of prosthetic ankle and natural ankle. Although the prosthetic ankle obtains a nice nonlinearity, it did not get adequate active behavior. A small area of active behavior can be observed at the top of the prosthetic torque-angle curve, but it quickly drops to the opposite side. If we define A_i (or B_i) to mean the energy generated (or dissipated) at the ankle and C_i to mean the total energy dissipated at the ankle in a gait cycle. The amount of the energy is calculated by the integral $E = \int \tau d\theta$, i.e., the area between the curves.

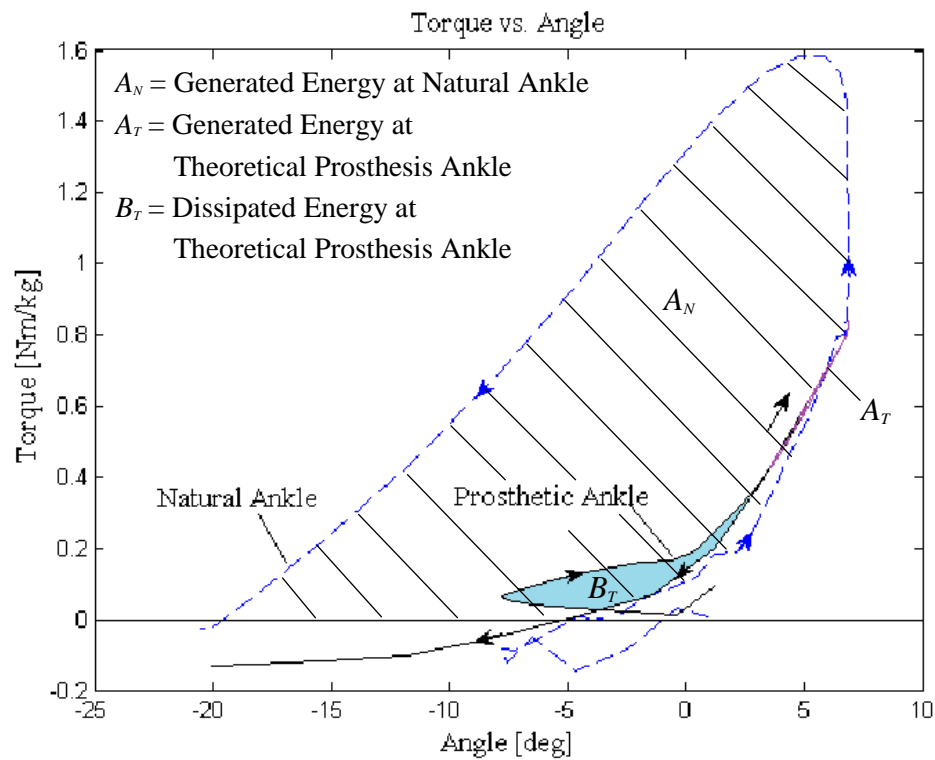


Figure 2.8 Torque-Angle Relationship of the Theoretical Prosthetic Ankle and the Natural ankle

In Figure 2.8, the lined area (A_N) represents that the average natural ankle generates $0.333 J/kg$ during push-off. As there is no energy dissipated during natural walking, C_N (total energy dissipated by natural ankle per gait cycle) is $-0.333 J/kg$. The shaded area (A_T) at the top of the prosthetic ankle curve means that the theoretical prosthetic ankle generates $1.91 \times 10^{-3} J/kg$ during push-off. The bottom shaded area (B_T) means that the

energy dissipated by the prosthetic ankle is $1.28 \times 10^{-2} J/kg$. Here, C_T equals B_T minus A_T , i.e., $1.09 \times 10^{-2} J/kg$ per gait cycle. The difference of total dissipated energy between natural ankle and theoretical ankle is $0.344 J/kg$ per gait cycle, which means that the theoretical ankle prosthesis dissipates more energy than natural ankle.

Although the theoretical prosthesis does not generate enough energy, it achieves a nice nonlinearity of ankle stiffness. The trend of the torque profile of the theoretical prosthesis is also similar to that of human ankle. An ankle prosthesis based on the parameters and results of the second optimization is designed in Chapter 3.

CHAPTER 3

Structural Design and Component Selection

In Chapter 2, the optimal spring rates and overall structure of the prosthesis were identified as part of conceptual design. This chapter presents the detailed design (3D model and material selection). Here, the developed CAD model is presented to communicate the prosthesis appearance.

With size as a design criterion, the structure is designed to be small. The material chosen for the structure is strong enough to achieve the requirements in the size and strength. Other components, such as bearings and springs, are reasonably sized and achieve the desired mechanical performance. Structural design and component selection were performed concurrently.

Section 3.1 presents the design of the main structure, i.e., the housing of the lower leg, the upper leg and the foot. Section 3.2 shows the spring selection and the design of the spring connections. Section 3.3 shows the design of the lock and unlock mechanism. Section 3.4 explains selection criteria for the bearings and other standard components. Section 3.5 shows the motion simulation and the motion limits. Section 3.6 identifies the fabrication cost.

3.1 Main Structure Design

The main structure here means the housing parts of the ankle prosthesis, which provide mounting bases for most of components and spring mechanisms. It includes the upper-leg, the lower-leg and the foot. This section introduces the models designed in NX 7.5 [21] and then explains the criteria for material selection.

3.1.1 Structure Design in NX

The size of the main structure determines the whole working envelope of the ankle prosthesis. According to design criterion 1, the ankle prosthesis should be designed small and compact in size. The optimized dimensions for spring positions are another constraint for the structure design. From the analyses presented in the last chapter, many components are located inside the main structure. Assume that all mechanisms work within the main structure in order to keep the ankle prosthesis compact and small. In this case, the spaces for the moving components and spring connections should be estimated and reserved. The dimensions of lower limb and theoretical mechanical model (Figure 2.3) are chosen as the starting point.

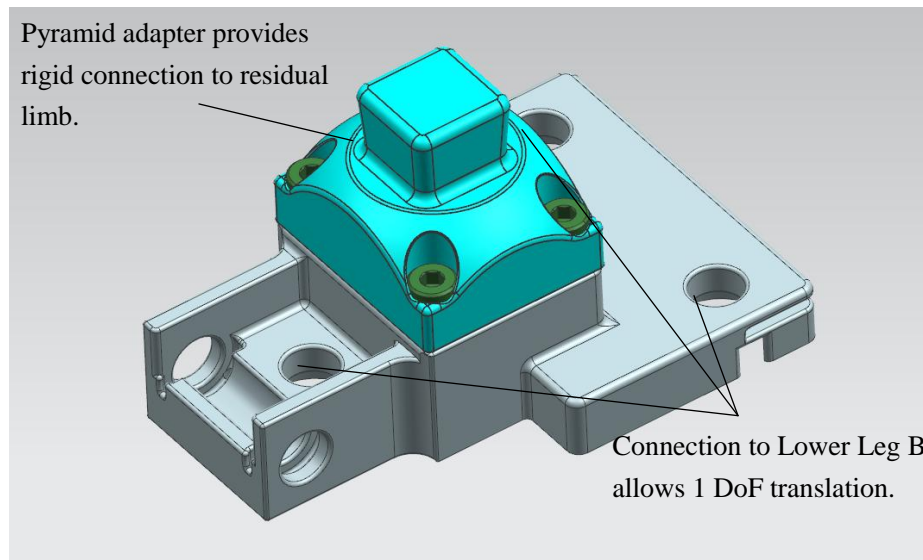


Figure 3.1 NX Model for Upper-Leg A

The upper-leg can move along the leg axis with respect of the lower-leg by spring mechanism k_I , which allows the DoF for leg translation of the prosthesis and helps the upper leg A move back to the original position. Three parallel springs are used to improve the stability of the upper leg. The three holes (in Figure 3.1) are used for the spring mechanism k_I , through which the upper-leg connects to the lower-leg and slides along the leg axis. Its top surface is connected to a pyramid adapter, which attaches to the

residual limb. A boss for the adapter and the detents in the back are designed to avoid interference with other components (shown in Figure 3.1). The pyramid adapter is commercially available. However, in this design, the available space on the upper-leg is too small to find a satisfactory commercial adapter. A pyramid adapter is designed to connect the residual limb and the ankle prosthesis.

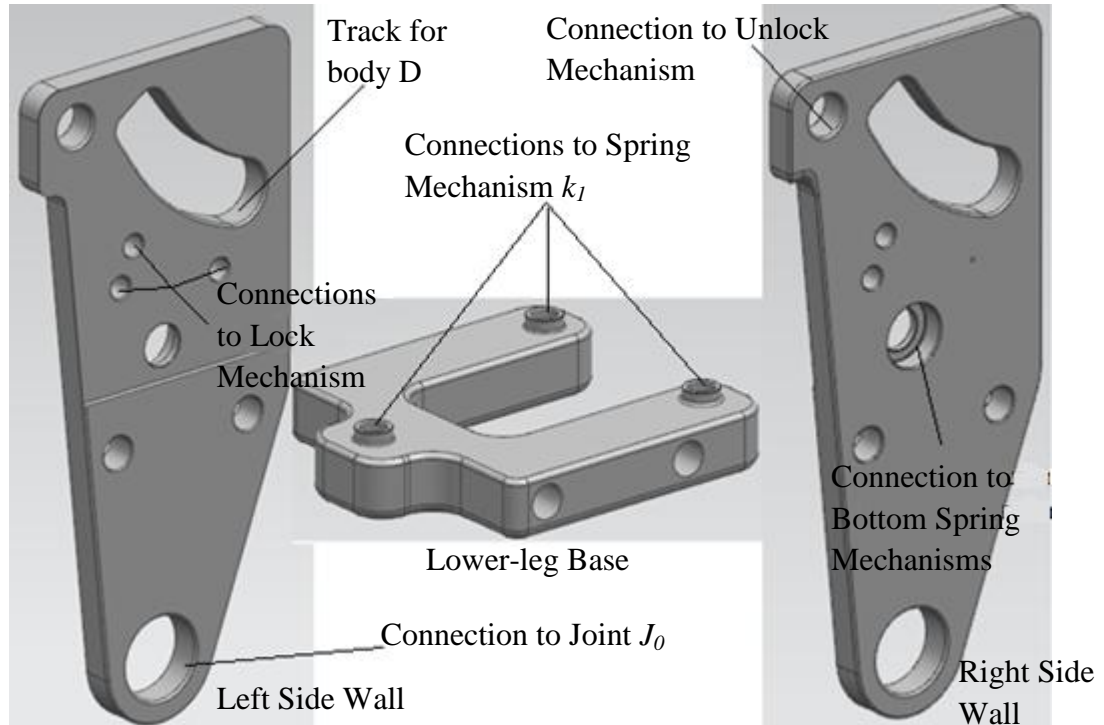


Figure 3.2 NX Model for Lower-Leg B

In addition to leg translation, the other DoF of ankle deflection should also be achieved by the main structure. The lower-leg acts as a supporting base and provides a rotating axis to obtain the adequate range of ankle deflection. Two separate parts are designed to obtain the functions of the lower-leg. One part allows the lower-leg to rotate about the axis perpendicular to the saggital plane by a revolute joint J_0 (represented the human ankle joint). The other offers support for spring mechanism k_1 to connect to the upper-leg by stainless steel shafts and external circlips. The rotating parts are called left or right side wall and the support part is called lower-base (shown in Figure 3.2). In addition to the ankle joint J_0 , the two side walls also provide space for mounting many

other mechanisms such as the inclined track for body D, the lock and unlock mechanism, and the bottom spring connection (ks_1 , ks_2 and ks_3).

The two side walls are connected to the lower-leg base using screws. The connection position (especially the height of the position) is chosen by considering the working envelope of springs and compactness. The material in the middle front of the lower-leg base is cut away to allow space for spring components k_2 and k_{s2} .

The foot C in this design consists of two sub-assemblies. They are made of different materials based on their different functions. One is the upper-foot where the ankle joint J_0 and spring connection positions are located; it is made of metal. The other is the lower-foot, which contacts the ground at the heel and forefoot; it is made of plastic. A toe joint is located at the forefoot in order to better match the human foot. Figure 3.3 shows the NX model for the foot.

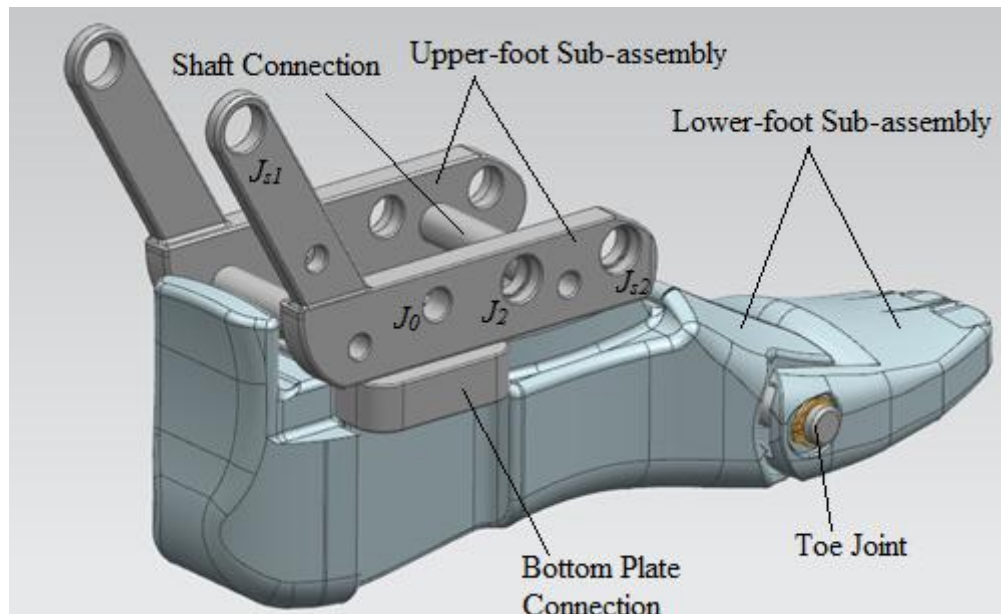


Figure 3.3 NX Model for Foot C

The upper-foot connects with the lower-leg through several spring mechanisms (ks_1 , ks_2 and ks_3) and through the ankle joint J_0 . The rotation between the upper-foot and the lower leg compresses the springs to generate the ankle torque needed for push-off. As shown in Figure 3.3, the upper-foot is made of two identical components linked together

with shaft connections and screws. The ankle joint J_0 and the Spring mechanism connections J_2 , J_{s1} , and J_{s2} are located on each side of the upper-foot.

The lower-foot is designed to resemble a human foot. It also offers a solid base for the prosthesis to lift the ankle joint J_0 to the height of human ankle. It has the roundness at the back part to aid the transition from heel strike to foot-flat, just like the human heel. A toe joint in the front is designed to allow the prosthesis roll over during push-off. A metal plate is used to connect the lower-foot and the upper-foot together by screws.

3.1.2 Material Selection

The materials of the main structure are chosen to be lightweight. All parts are designed to satisfy the requirement for strength to guarantee repeatability and safety. The main structure acts as the supporting base and has the highest weight in this ankle prosthesis. A lightweight material (aluminum 6061, density 2.7 g/cm^3) was selected to reduce the weight. It is commonly used for structural components and offers good strength-to-weight ratio with good corrosion resistance.

Compared to other parts, the lower-foot component of the foot C has less strength requirement and more complicated shape. ABS plastic (density 1.05 g/cm^3) was selected because it is easily and quickly machined. Mechanical properties of aluminum 6061 T6 and ABS plastics are presented in Appendix A.1.

3.2 Spring Selection and Spring Connection Design

This section mainly states the criteria used in spring connection design and spring selection. The process of spring connection design and spring selection is simple but time-consuming. Using the optimal spring stiffness provided in Section 2.4 as a starting point, the major considerations are that the springs must have the required deflections and be in reasonable sizes to keep the prosthesis small and compact. The selection cannot be completed without considering the working envelope constrained by the housing and

spring selection affects the design of the housing. The spring sizes directly affect the sizes of the spring mechanisms; and in turn, the distance between the spring connections (decided by mechanical dimensions in Table 2.1) will affect the selection of the spring. As such, several iterations of spring selection and structure refinement were performed.

3.2.1 Spring Selection

Springs, through which energy is stored and released to mimic human ankle functions, are the most important components in this design. The configurations of the springs affect the performance of the ankle prosthesis. All springs discussed below are conventional (helical) compression springs.

All spring stiffness and connection geometries were determined by the second optimization (shown in Table 2.1). The maximum free lengths of the springs are the distances between corresponding connection points. Some spring rates are very large but the maximum free length is relatively small. The first challenge of spring selection is to find a manufacturer that stocks appropriate springs having the required range of stiffness within proper sizes. Although customized springs are available for purchase, the cost is very high relative to standard springs.

Table 3.1 Geometry Values for Springs

Spring	Maximum Length (<i>mm</i>)	Minimum Deflection (<i>mm</i>)	Minimum Length of Connection Mechanism (<i>mm</i>)
k_1	98	12	98
k_2	101.5	24	111.7
ks_1	60	24.9	80.6
ks_2	82.8	15.6	98.7
ks_3	73.0	5.8	98.7

During the operation of the ankle prosthesis, the springs will be compressed to store energy. The range of human ankle deflection is used as the range of motion for the ankle prosthesis. To store enough energy, the springs should be at least compressed to the

minimum deflection. With constrained maximum free length, the compression ratio (free length/ solid length) is relatively large. Only a few springs satisfy this requirement, which brings the second challenge of spring selection. The configurations and the minimum deflections of the springs are presented in Table 3.1.

After analyzing the general dimensions of the springs, the next step is to check the commercial availability. Among all the spring manufacturers evaluated, Century Spring Corp (CSC) offered the largest stock spring selections and the most detailed product information. The characteristics of the selected springs are listed in Table 3.2. The spring rates are within 5% percent deviation of the optimized values.

Table 3.2 Spring Characteristics for Human Subject Testing

Spring	Quantity	CSC Stock Number	Spring Rate (N/mm)	OD (mm)	ID (mm)	Free Length (mm)	Solid Length (mm)	Maximum Deflection (mm)
$k_{1, front}$	2	3851	4.0	14.3	11.1	38.1	14.2	23.9
$k_{1, back}$	1	K-56	9.6	12.7	9.0	38.1	20.1	18.0
$k_{2, top}$	1	S-1332	74	15.5	9.9	28.7	15.5	13.2
$k_{2, bottom}$	1	Q-75	110	12.2	6.6	38.1	25.7	12.4
ks_1	2	11390	4.9	13.5	10.2	41.4	18.3	23.1
ks_2	1	10416	128.8	17.4	9.9	46.0	30.0	16.0
ks_3	1	W-71	28.2	8.0	4.8	22.4	15.0	7.4
k_{lock}	2	S-1420	1.2	7.5	6.3	14.2	3.6	10.6
k_{top}	3	K-44	14.7	11.5	9.0	7.9	4.3	3.6

The spring rate for k_1 is achieved by using three springs to increase the support stability of the lower-leg and share the load from the upper-leg. Two of the springs are located in front part of lower leg and the other located at the back. To maintain balance in the upper-leg support, no extra moment about the ankle axis should be generated while the upper-leg slides and compresses the spring set k_1 . Due to constraint on the distances between the spring connections and the ankle axis, the back spring should be about 2.5 times stiffer than the front one. In this case, the split spring rates are calculated as 4.0 N/mm for spring $k_{1, front}$ and 9.6 N/mm for spring $k_{1, back}$.

The spring k_2 was divided into two parts as well because no single in-stock spring was adequate (i.e., satisfied the theoretical spring rate and the required minimum deflection at the same time). Spring $k_{2, top}$ and spring $k_{2, bottom}$ are connected in series. The spring rates of the two springs should be close to each other, but the size (diameter) of spring $k_{2, bottom}$ should be smaller than spring $k_{2, top}$ to avoid interference with bottom spring sets ks_2/ks_3 . Spring $k_{2, bottom}$ connects with spring $k_{2, top}$ parallelly but eccentricly. Spring ks_3 is connected eccentricly within spring ks_2 , which requires that the outer diameter of spring ks_3 should be smaller than the inner diameter of spring ks_2 . Springs k_{top} are used to reduce the impact forces when the upper leg rapidly returns to the neutral position. They are chosen to have the same stiffness with spring k_1 . Springs k_{lock} are used to prompt the lock mechanism to lock body D.

3.2.2 Design of Spring Connection Mechanisms

This subsection illustrates the design results for spring connection mechanisms (for spring sets k_1, k_2, ks_1 and ks_2/ks_3). The mechanism design and the spring selection are conducted simultaneously.

The connection mechanisms are designed to support the springs and guide them along the right directions. Most movement occurs between the springs and spring connection mechanisms. To increase the work efficiency and obtain quiet operation, the friction between moving parts should be minimized. According to [22], the coefficient of friction between aluminum and aluminum (1.05 – 1.35) is almost ten times larger than that between steel and steel (0.14). In order to achieve low friction and improve the performance of ankle prosthesis, stainless steel was chosen as the material for the spring connection mechanisms.

Stainless steel 303 (bearing shaft, density 7.9 g/cm^3) was used to get the required properties of low friction and high strength. Stainless steel 303 is austenitic steel with a polished surface, ideal for moving parts. Stainless steel 316 (density 8.03 g/cm^3) was used

for most supporting parts because of its high strength. Mechanical properties for Stainless steel 303 and 316 are listed in Appendix A.1.

The designs for spring connection mechanisms are presented in Figure 3.4 and Figure 3.5. The dimensions for these mechanisms are mainly constrained by the optimized geometry dimensions and the selected spring characteristics. The stainless steel shafts shown in the figures correspond to the various joints that connect the main structure and spring mechanisms. During operation of the prosthesis, the shaft of joint J_2' connects and slides together with body D in the track on lower-leg. An extra pair of bearings is added on the shaft of joint J_2' to unilaterally connect with the upper-leg and reduce the energy lost when the spring k_2 is compressed. The selection for bearings and other components shown in the figures will be explained later.

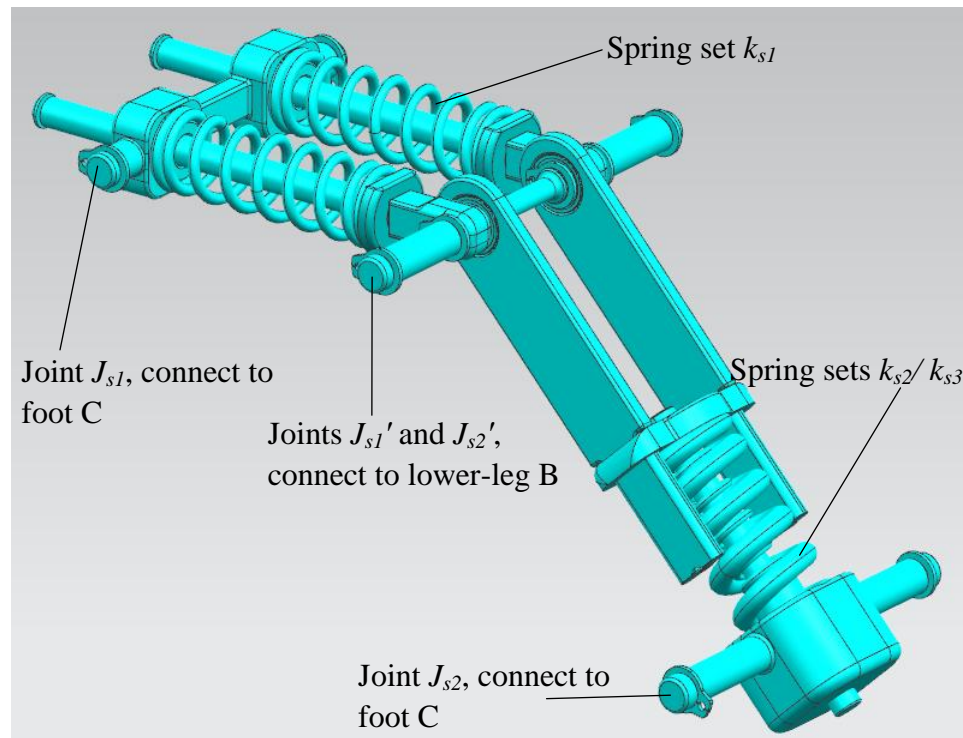


Figure 3.4 Spring Mechanisms of k_{s1} and k_{s2}/k_{s3}

After completing the designs of main structures and spring mechanisms, a preview for those assembled parts is available in NX to check the available space for other components. As the spring mechanisms are close to each other, an interference check was conducted.

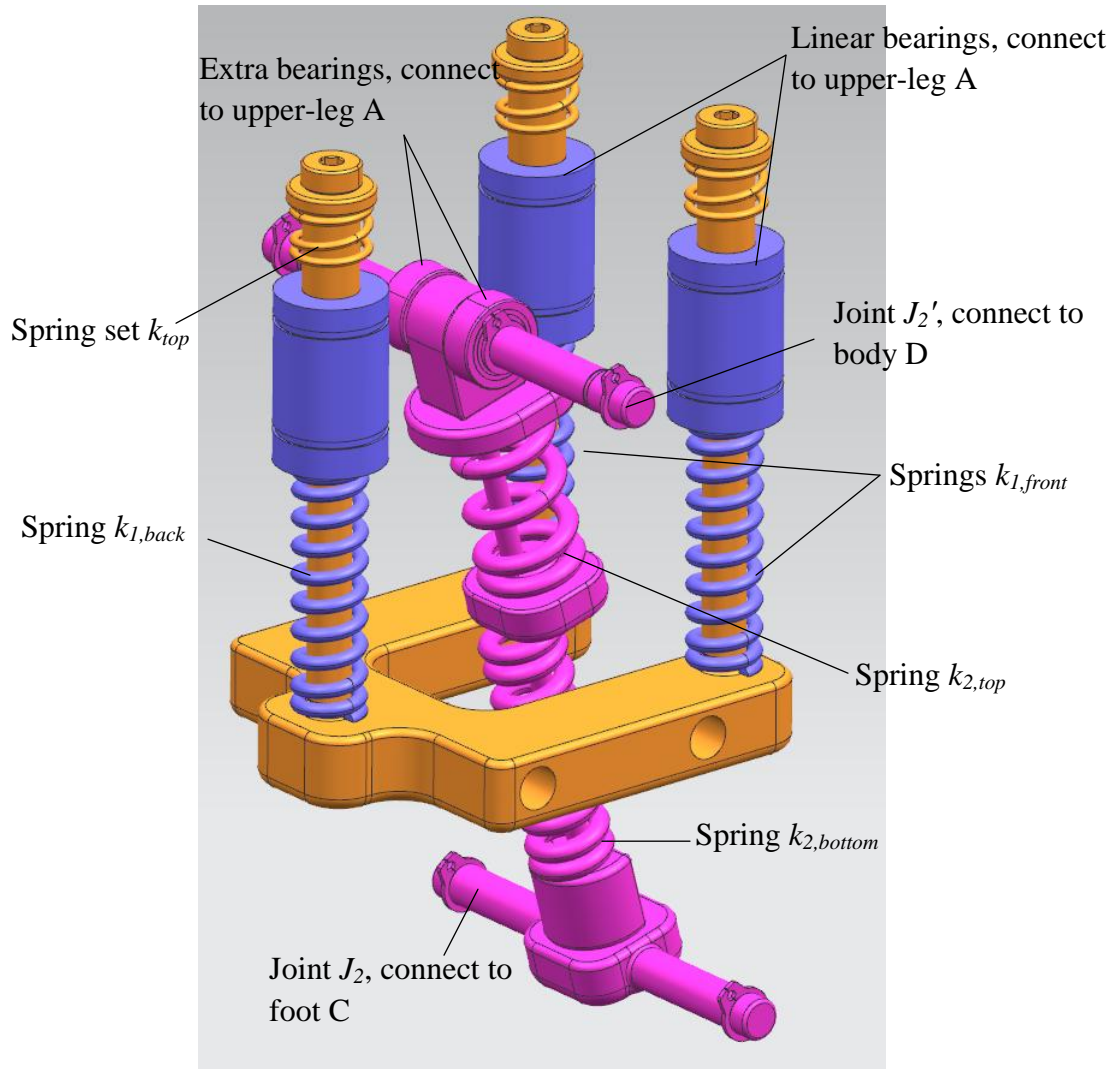


Figure 3.5 Spring Mechanisms of k_1 and k_2

3.3 Design of Lock and Unlock Mechanism

To further achieve a torque profile similar to that of a natural ankle (the nonlinearity), this prosthetic design uses the lock and unlock mechanisms. The lock mechanism is designed to retain the energy stored in spring k_2 so that the prosthesis can provide adequate torque about ankle joint for push-off. As shown in Figure 3.6, body D and spring k_2 are connected to the same shaft. The shaft of joint J_2' and body D are unilaterally connected to the upper-leg, which allows the shaft and body D to be locked while the upper-leg moves back to its equilibrium position. When body D reaches the lock position

of the sliding track (the track is 2 mm longer for overtravel), the lock mechanism blocks shaft of joint J_2' from returning to its equilibrium position. The shaft and related components (body D and spring k_2) are held until the unlock mechanism is triggered. Figure 3.6 and Figure 3.7 show the positions of related components in the lock and unlock situations. Two sets of lock and unlock mechanism are designed on both left and right side walls.

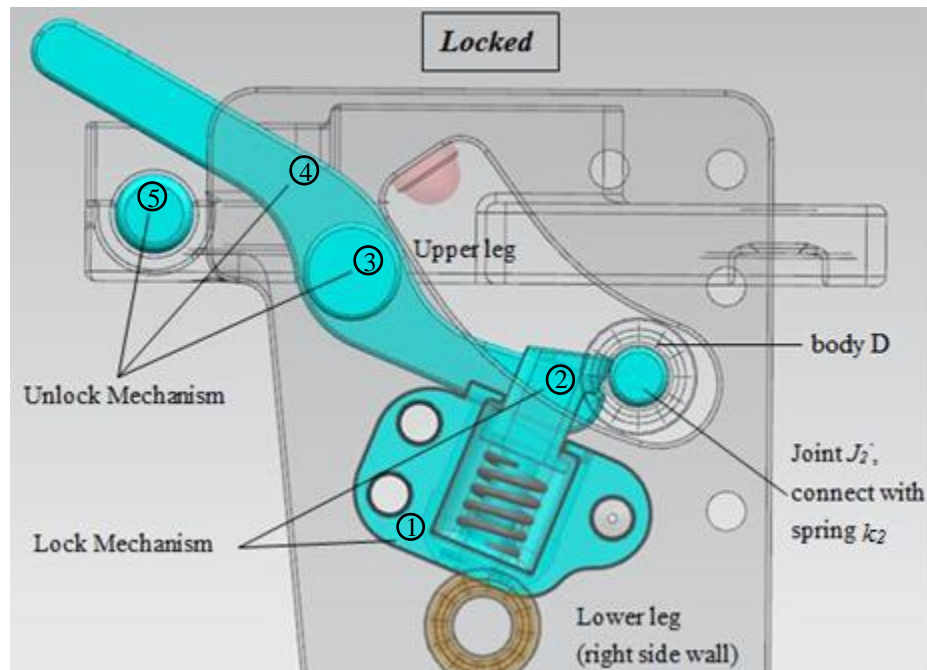


Figure 3.6 Locked Situation

The lock mechanism consists of two parts: lock container (Part 1 in Figure 3.6) and lock slider (Part 2). The lock container is attached to the left and right side walls of the lower leg by screws. The lock slider is located inside the lock container and connects with the unlock mechanism through a unilateral slide joint (only engaged in the direction of pushing the slider down). Similarly, a lock spring k_{lock} is used to connect the two lock parts. The lock spring is used to push the slider up to lock the shaft of joint J_2' . The lock slider also has a smooth top surface, which allows the shaft of joint J_2' to glide over to reach the lock position.

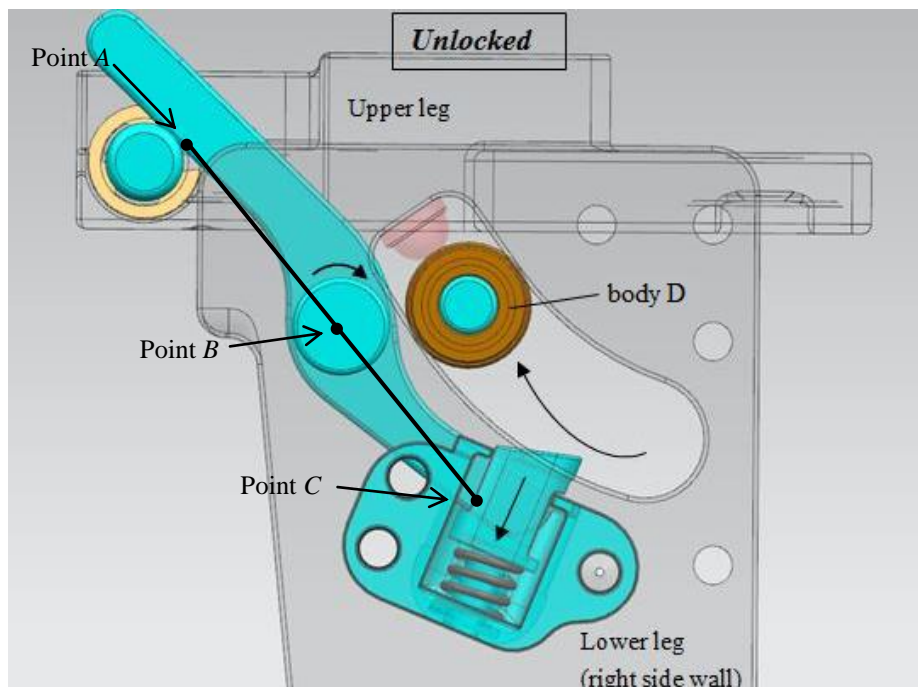


Figure 3.7 Unlocked Situation

The unlock mechanism consists of three parts: the connecting bar (Part 3 in Figure 3.6), the unlock piece (Part 4) and the unlock pin (Part 5). The connecting bar is the pivot of the unlock piece. The unlock piece attaches to the left or right side wall and connects with lock mechanism and the unlock pin unilaterally. The unlock pin moves together with the upper-leg. In order to unlock the shaft of joint J_2' simultaneously, a single unlock pin is used for both left and right mechanisms. The unlock position is the equilibrium position of the ankle prosthesis. In Figure 3.7, point B represents the pivot center of the connecting bar; point A represents the contacting point between the unlock piece and the unlock pin; point C represents the contacting point of the unlock piece and the lock mechanism. In order to release lock mechanism efficiently, the distance between point A and B should be equal or longer than the distance between B and C according to principle of leverage. As stated previously, the prosthesis should return to its neutral position just after push-off, which means that the unlock mechanism is designed to release body D and the shaft of J_2' at the end of push-off.

As the lock and unlock mechanism are located very close to many other components (spring mechanisms, upper-leg and body D), the sizes of the lock and unlock components are constrained. However, as moving parts, the requirements for strength and low friction should also be satisfied. Both lock and unlock mechanisms are made of stainless steel to achieve those requirements. The shapes of the components are carefully designed to ensure that no interference exists between the components.

3.4 Selection of Bearings and Other Conventional Components

Bearings and other conventional components are used throughout the mechanism. This section presents the selection results for the bearings, internal helicoils and external circlips.

Bearings

Two types of bearing are used in this design: ball bearings and linear plain bearings. Ball bearings are used in most of the rotational joints. The bearings are mainly located in main structure and spring mechanisms. For compactness, the space for bearings is limited. To meet these constraints, the best choice was miniature deep groove ball bearings, which are durable, quiet and lightweight.

Linear plain bearings are used to connect the upper leg to the lower leg. They are used to provide a smooth and low-friction linear sliding along the axis of spring k_1 (shown in Figure 3.6). DryLin R linear bearings from IGUS Company satisfy both size and mechanical properties. The properties for the ball bearings and linear bearings are listed in Appendix A.1.

Helicoils and External Circlips

Screws are used as the primary connection method in this design. However, many connections join aluminum or plastic parts to other parts. Aluminum and plastic are relatively soft materials compared to stainless steel. If screws are inserted directly into aluminum or plastic, there exists the risk that the interior threads would be stripped,

especially when there is axial load. Helicoils are used to provide durable threaded holes in a soft material. Helicoils usually work together with specific screws. Metric screws M4, M5 and M6 are used in this design.

External circlips are another type of fastener elements which are usually inserted into machined grooves on shafts or dowel pins. They allow rotation but prevent axial movement. In this design, circlips are mainly used at the end of shafts to prevent axial movement of bearings or other components. They are selected according to the diameters of the supporting shafts. In this design, the external circlips for 4 mm, 6 mm and 8 mm are used.

3.5 Motion Simulation

Although interference analysis is conducted each time a part of the prosthesis is completed, it can only identify geometric conflict for a single configuration. During the operation of the ankle prosthesis, the positions and relationships of moving parts change. To check the clearances throughout the operation, a motion simulation was performed. It provides a visual for the way that the prosthesis ankle will move during walking. Figure 3.8 shows the link representations for designed ankle prosthesis in motion simulation. Link 1, 2 and 8 are the foot C, lower-leg B and upper-leg A. Link 9 and 11 represent the unlock piece and the lock slider, which are main working parts of lock and unlock mechanisms. The other links represent spring mechanisms. To simplify the simulation, the foot C (link 1) is specified to be fixed to the ground. All the joints assignments and simulated movements are based on motion relative to this fixed link.

The results of motion simulation are important for revisions of the component designs. Note the circled places in Figure 3.9, where little clearance is designed between the main structure and the spring mechanisms. Geometric conflicts were identified during motion simulation between spring mechanism k_2 and spring mechanism ks_2/ks_3 . To

reduce the interference, these springs are set off from their line of action. All modifications were made in NX before fabrication.

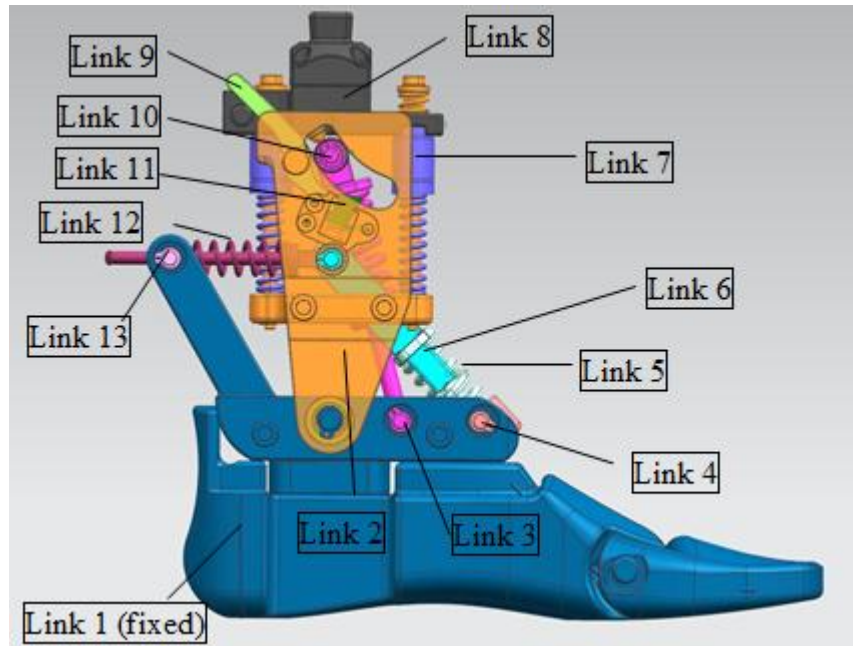


Figure 3.8 Representations of Motion Simulation Links

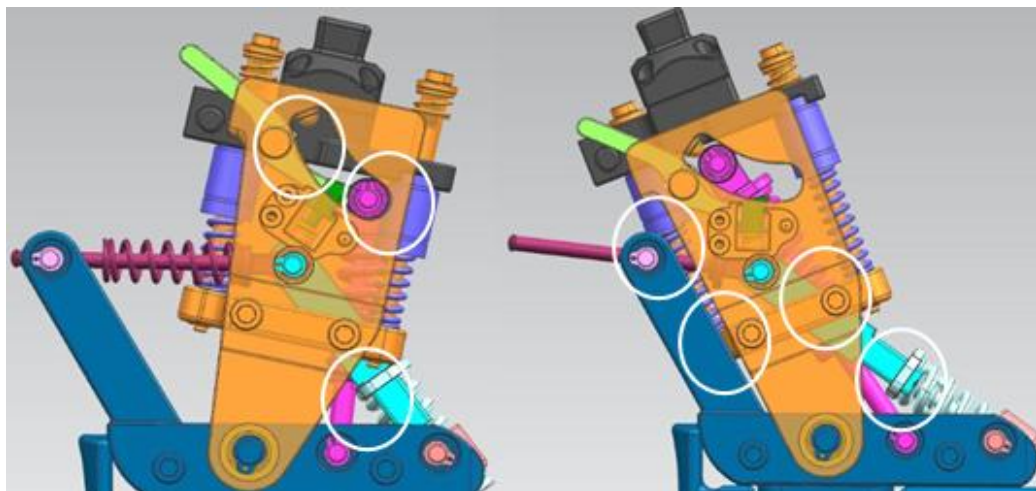


Figure 3.9 Modifications of the Prosthesis

3.6 Fabrication of the Ankle Prosthesis

The prosthetic design in CAD software was completed after the motion simulation. To further verify the ability of the prosthesis, real-world testing will be performed. The

Nielsen Company was selected to fabricate the custom components of the prosthesis. The cost for custom components of one designed prosthesis is \$7,641. The detailed bills for the designed and commercial components are available in Appendix A.2

Although there are more than thirty parts in the prosthesis, the assembly takes less than half a hour. The order of assembly is similar to the sequence of the link number shown in Figure 3.8, except that link 8, link 2 and link 1 are in the last three assembled components. Lubricating grease is used to reduce the friction between components.

CHAPTER 4

Ankle Performance Evaluation

After the motion simulation was completed, the kinematic performance of the prosthesis was verified. Both robot tests and human subject tests were performed on the designed prosthesis. Although the tests were conducted to verify theoretical performance of the optimized device, the physically realized prosthesis was somewhat different (different spring rates and additional components were used).

This chapter presents the performance evaluation of the designed ankle prosthesis. Section 4.1 first introduces the robot testing configurations and then provides the results from the robot tests. Section 4.2 explains the human subject testing methods used in the gait lab and provides an analysis of the test results. Section 4.3 summarizes the test results and the overall performance of the prosthesis.

4.1 Robot Testing

Before testing the prosthesis on human subjects, preliminary robot tests were conducted to verify the ability of the prosthesis to generate adequate ankle torque during the stance period. Another reason for robot tests was to ensure the structural integrity of the device for the safety of human subjects testing.

The prosthesis was instrumented to measure motion along the leg and motion about the ankle. Forces and torques were also measured in robot testing. A detailed description of the test apparatus and procedures are provided before the evaluation of test results.

4.1.1 Robot Testing Configuration

Robot testing configurations include hardware modifications, i.e., spring selection, adapter designs, and software preparation such as robot and LabView programming.

Springs

Due to the nominal payload of the robot (12 kg), springs stiffness were scaled down to 25% of the optimized values. Corresponding springs were selected from Century Spring Corp to satisfy the same geometry requirement identified in Table 3.3.

The characteristics of the springs used in robot testing are listed in Table 4.1. A single spring was used as spring k_2 in robot test because the minimum deflection can be satisfied. The space reserved for spring $k_{2, bottom}$ was replaced by an aluminum tube. The tube was used to lift the spring k_2 to a position without interference with the spring mechanism ks_2/ks_3 . Spring k_{lock} and spring k_{top} have the same rates as the original springs.

Table 4. 1 Spring Characteristics for Robot Testing

Spring	Quantity	CSC Stock Number	Spring Rate (N/mm)	OD (mm)	ID (mm)	Free Length (mm)	Solid Length (mm)	Maximum Deflection (mm)
$k_{1, front}$	2	71482	1.1	12.2	10.3	38.1	7.4	30.7
$k_{1, back}$	1	S-1129	2.6	14.3	11.2	38.1	16	22.1
k_2	1	71825	13.2	15.24	10.9	44.5	20.3	24.2
ks_1	2	71497	1.3	13.5	12.2	41.4	9.4	32
ks_2	1	3057	37.7	15.1	9.7	41.4	24.1	17.3
ks_3	1	70973S	7.5	7.6	5.2	25.4	12.7	12.7
k_{lock}	2	S-1420	1.2	7.5	6.3	14.2	3.6	10.6
k_{top}	3	K-44	14.7	11.5	9.0	7.9	4.3	3.6

Adapters for Robot and Sensors

A Staubli RX 130 6-DoF robot with CS7 controller was used. An ATI 6-axis sensor was used to obtain the force and torque data. Because the ankle angle-torque relationship is an important aspect of the prosthetic ankle performance, the prosthesis was instrumented to measure the motion. A linear potentiometer and a rotary potentiometer are used to obtain the linear deflection along the leg and the rotary angle about the ankle respectively.

In order to connect the prosthesis with the robot and sensors, various adapters were designed. The adapters for the robot and the Force/ Torque sensor are located at the top

of the prosthesis. A conventional dual adapter is used to attach the fabricated prosthesis to the robot. The calibrations for potentiometers and the data interpretation method are presented in Appendix B.1.

Robot and LabView Programing and Testing

The CS7 controller of the robot uses V+ programming language. Through programming, the trajectory of the robotic arm was specified. The robot testing is focused on the stance period (0–62% of the gait cycle). One stride is tested in each trial. At the end of the program, the robot arm returns to its starting position. The smooth trajectory of human fibula joint during walking (Figure 4.1) is used as initial controlling points of the robot. It is obtained by averaging multiple fibula walking trajectories.

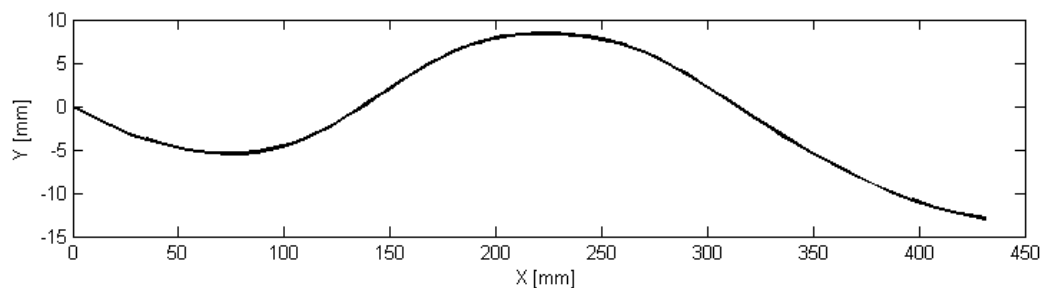


Figure 4.1 Walking Trajectory of Human Fibular Joint

To acquire data from various sensors, Hyper Terminal and LabView are used. The Hyper Terminal is a communication software that is used to connect and transfer information between the *F/T* sensor and computer using serial COM ports. In this testing situation, it was set for a baud rate of 115200 and 8 data bits. The frequency of the DAQ assistant in the LabView program was 114 *Hz*.

Figure 4.2 shows the instrumented prosthesis mounted to the robot with all the additional adapters and connections. Additional leg connections were used to obtain a better alignment between the upper-leg and the lower-leg. After finishing the assembly and the robotic programming, the ankle prosthesis was ready for testing. The robot testing protocol is shown in Appendix B.2.

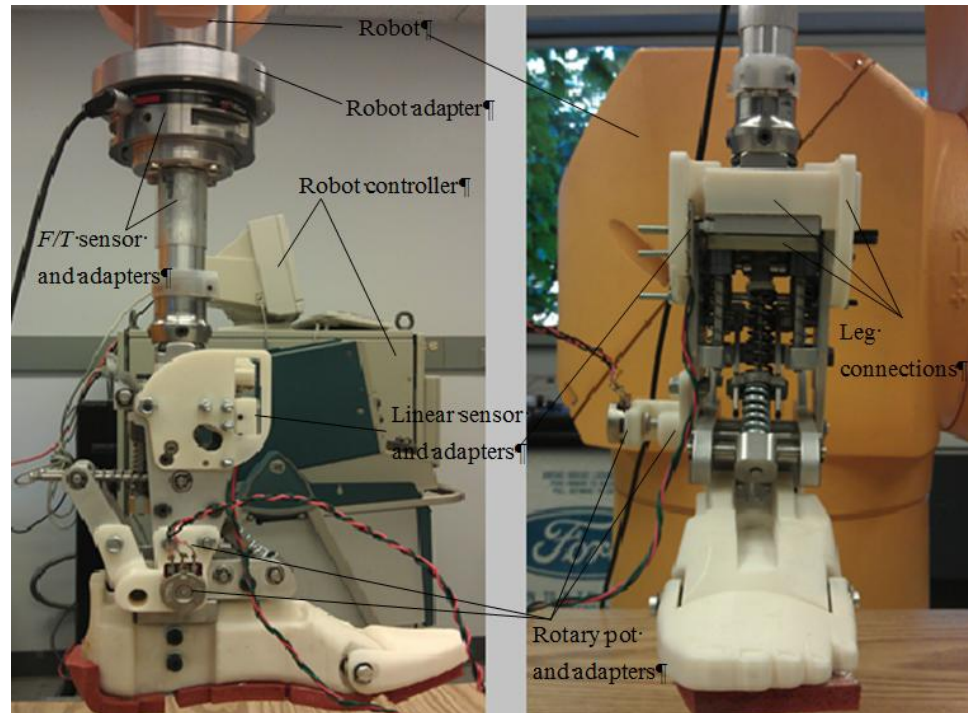


Figure 4.2 The Fully Assembled Prosthesis Mounted to the Robot with All Add-ons

4.1.2 Results and Analysis from Robot Tests

The raw data obtained from the sensor are not the kinematic or kinetic values needed for comparison to desired performance. Calibrations were taken before the test for data interpretation. The interpreted results are analyzed in MATLAB. The average human ankle performance (obtained by Winter [5]) was used as a benchmark for comparison.

Robot Testing Results and Analyses

The test results are analyzed in two aspects:

1. The results are compared between each test trial to confirm the repeatability of the prosthesis (results are presented in Appendix B.3).
2. The results are compared with the theoretical results and the results for a natural ankle [5]. The purpose of this comparison is to check whether the designed prosthesis achieves the design objectives.

Three parameters (the ankle angle, the ankle torque and the force along the leg) are used in the comparison of performance. The ankle angle indicates the kinematic performance. The ankle torque and the force along the leg indicate the kinetic performance. The active behavior will be evaluated using the torque-angle relationship.

The results of each test trial (in Appendix B.3) for robot testing show that the test apparatus and the prosthetic ankle have a good repeatability. In Figure 4.3 – 4.6, the average result of the robot test is compared to the normal human ankle data (obtained by Winter [5]) and the theoretical performance of the prosthesis. The “Prosthesis” curves represent the average test results for the designed ankle prosthesis, the “Human Ankle” curves and the “Theoretical” curves represent the average human ankle data and the theoretical prosthetic ankle data. In Figure 4.3 and Figure 4.5, the “Human Ankle” curves and the “Theoretical” curves are the same because the two parameters (ankle angle and ankle force) were used as input in the optimization.

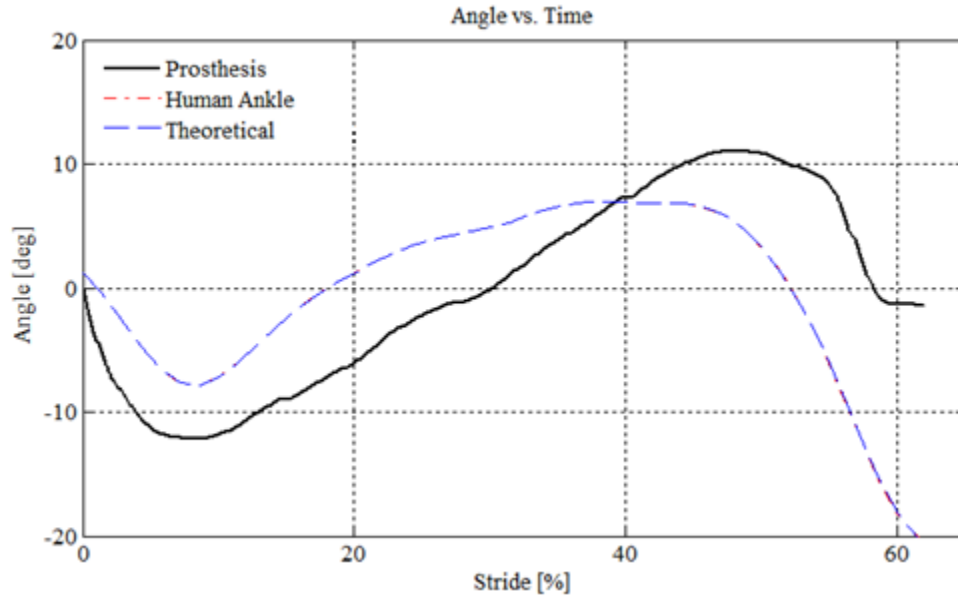


Figure 4.3 The Average Ankle Angle for Robot Test and Comparisons

Figure 4.3 indicates that the prosthesis has larger plantarflexion and dorsiflexion during the stance period but very little plantarflexion during push-off (end of the stance period). Peak dorsiflexion occurs later in the gait cycle.

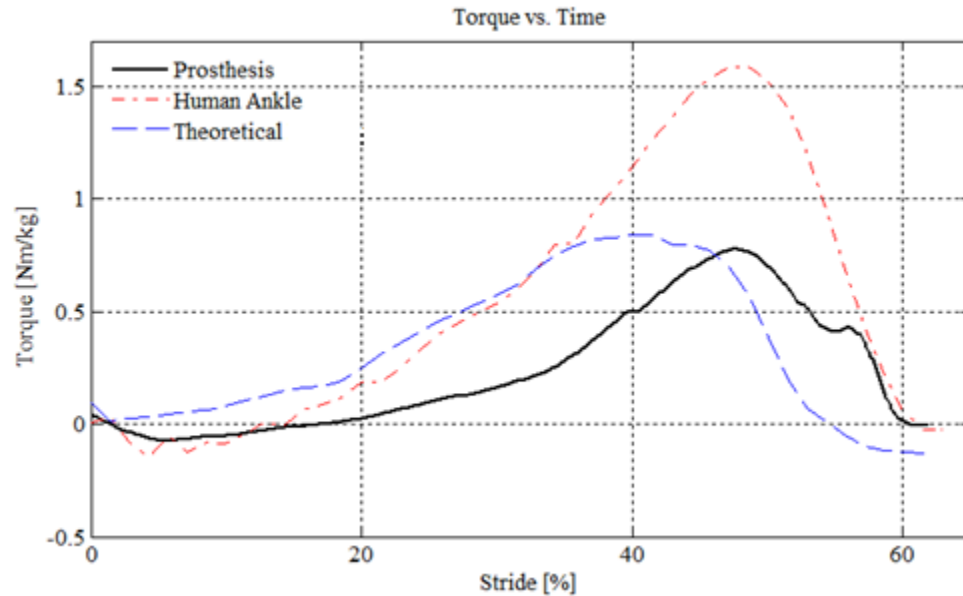


Figure 4.4 The Average Ankle Torque for Robot Test and Comparisons

The ankle torque profiles illustrated in Figure 4.4 shows more differences than the angle profiles. Both the prosthesis results and theoretical results have lower peak values (47% less). The robot test results are better than the optimized result. That is because the ankle angle increases more slowly than that for normal human ankle. A small increase occurs at the end of the stance period. It is caused by the significant small plantarflexion. The ankle torque turns down because that the spring k_2 is gradually released and that the prosthesis slightly rotates to plantarflexion angle (about 2° as shown in Figure 4.4) and generates a balance torque. When the prosthesis stops rotating backwards, the ankle torque reduces only because of the spring releasing and the rate suddenly reduces.

The average ankle force of the prosthesis is compared with that from human ankle in Figure 4.5. The second peak matches human ankle behavior better than the first one. The first peak happens 7.5% later and 25.7% lower than a natural ankle. The second peak,

however, occurs at about the same time with similar value. This may be caused by the larger plantarflexion angle.

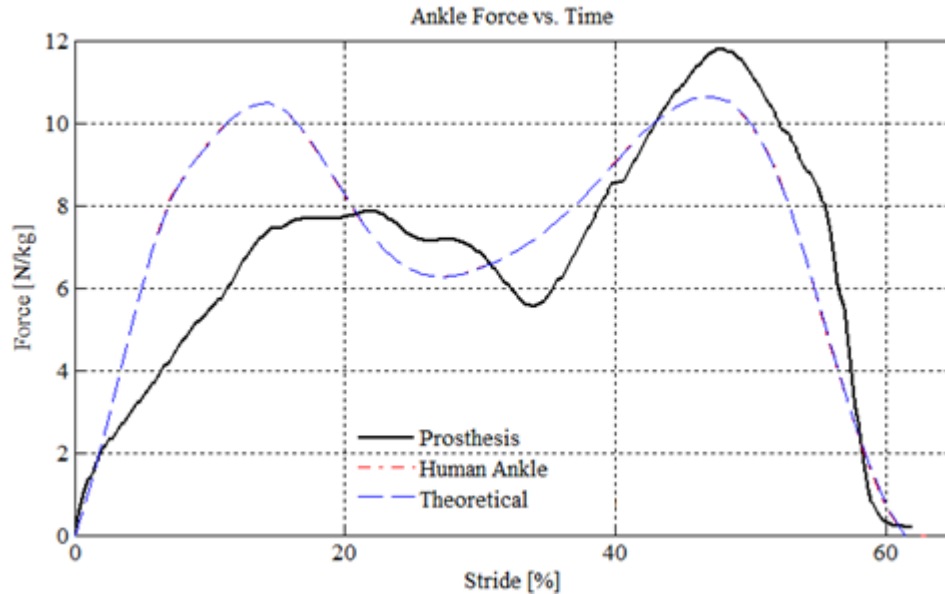


Figure 4.5 The Average Ankle Force for Robot Test and Comparisons

Figure 4.6 indicates that the torque-angle relationship of the prosthesis and theoretical are similar. The prosthesis test result is flatter because the designed prosthesis provides a smaller ankle torque with a larger ankle deflection. However, the normal human ankle shows a much more active behavior than either of the other two.

The lined area (A_R) indicated that the energy generated by the prosthesis test was $6.61 \times 10^{-3} J/kg$. The shaded area (B_R) indicated the ankle prosthesis dissipated $7.76 \times 10^{-3} J/kg$ during push-off at each gait cycle. Although a larger amount of energy was generated at the prosthetic ankle compared to the theoretical result, it still generated less energy than its dissipation (no active behavior) in a gait cycle. The total dissipated energy (C_R) of the prosthetic ankle was $1.15 \times 10^{-3} J/kg$ per gait cycle. The difference of total dissipated energy between the robot testing result and the theoretical result was $-1.79 \times 10^{-2} J/kg$ per gait cycle, which means that the prosthetic ankle dissipated less energy in the robot testing. It also can be observed that a larger amount of energy is

generated ($A_R > A_T$) in the robot testing, which means that the prosthetic ankle works better than expectation (theoretical result).

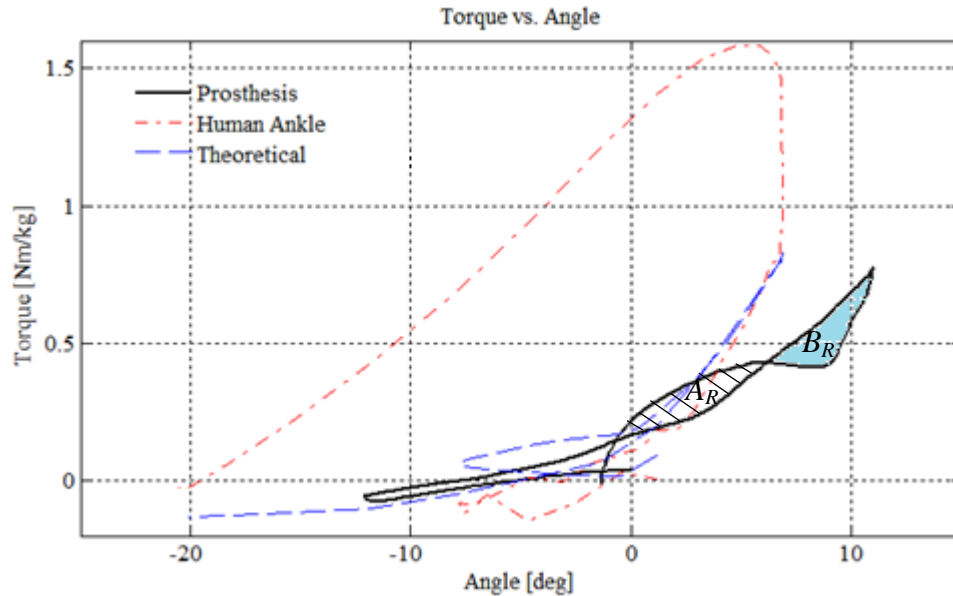


Figure 4.6 The Torque-Angle relationship for Robot Test and Comparisons

4.1.3 Conclusion

The major advantage of the robot testing is that we can accurately control the movement of the prosthesis. The comparison of test results show that the designed prosthesis has a very good repeatability. Results confirm that the lock and unlock mechanisms work smoothly; and the device properly returns to the neutral position at the end of the stance period. However, the mechanical objectives to generate adequate ankle torque and to obtain active behavior similar to that of a natural ankle are not achieved. The torque generated by the ankle prosthesis, although close to the theoretical performance for the device, is inadequate.

Although the robot tests are not as successful as desired, they provide an insight of the capabilities of the prosthesis. After the robot tests, no component were damaged. The prosthesis demonstrates its ability to operate in a way similar to that of a human ankle.

4.2 Human Subject Testing

Robot testing showed that the designed prosthesis has structural integrity and proper operation. To validate the ankle prosthesis, human subject tests were also conducted. This subsection describes the methodology of human subject testing and evaluates the test results.

4.2.1 Human Subject Test Method

The human subject test is performed at Orthopaedic & Rehabilitation Engineering Center (OREC) in Milwaukee. A unilateral (left) below-knee amputee weighting 104.5 (kg) was used in this study. The subject walked along a path at his normal walking speed.

Reflective markers were placed bilaterally on the posterior and anterior superior iliac spine, hip joint, knee joint, ankle joint and toe joint for the system to obtain data. The kinematics data was acquired by VICON system; the ground reaction forces were acquired by force plates. The subject must fully step on the force plate to get good force data. Software associated with VICON system was used to calculate the torque and power for each joint by the force and kinematic data. System calibrations were conducted before and after the subject tests. The subject was accompanied within a reachable range during the whole testing period.

4.2.2 Test Results and Analysis

The analysis of the human subject test results is similar to that for the robot testing results. The ankle angle, the ankle torque and the force along the leg were used in evaluating the performance. Human subject test results were compared to the theoretical results, the robot test results, the subject's healthy leg results, and natural human results [5]. The figures that show the comparisons between each successful test trial are

presented in Appendix C. Similar to the results of each trail in the robot testing, the human subject test results validated the repeatability of the ankle prosthesis.

In Figure 4.7 to Figure 4.10, the average human subject results are presented and compared to various other results. The curves of “Prosthetic Leg” represent the test results of human subject with the designed ankle prosthesis; the curves of “Healthy Leg” indicate the test results of human subject with his healthy leg; the curves of “Human Ankle” represent results of the natural human ankle; the curves of “Theoretical” are the theoretical results of the designed prosthesis in the optimization; the curves of “Robot Test” represent the robot testing results. In Figure 4.7 and Figure 4.8, the “Human Ankle” curves and the “Theoretical” curves are the same because the ankle angle and force of human ankle were used as inputs in the optimization.

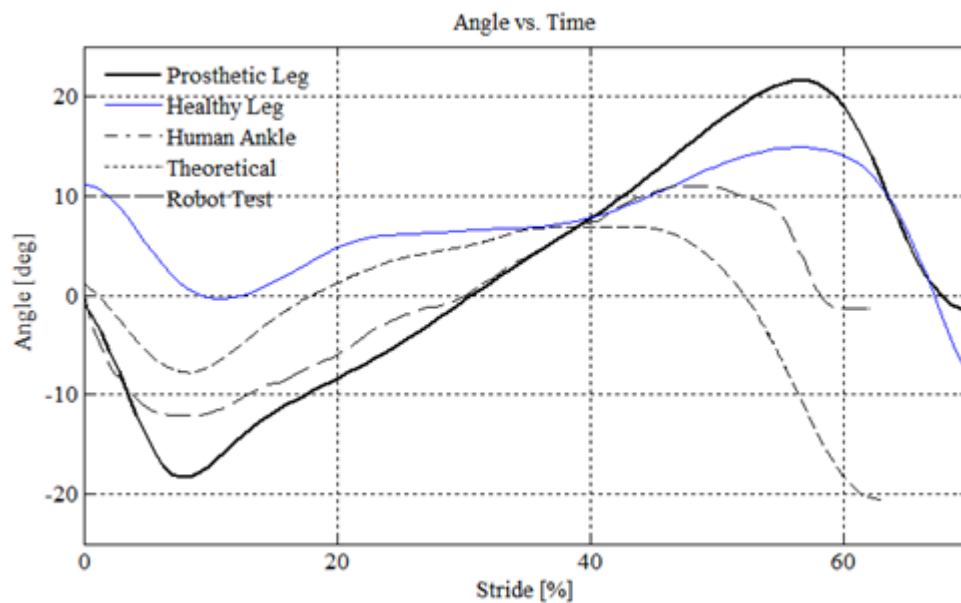


Figure 4.7 The Average Ankle Angle for Human Subject Test and Comparisons

The ankle deflection profiles presented in Figure 4.7 show the relations between each set of result. The result of the prosthetic leg had a similar shape with the robot testing result (larger dorsiflexion angle and no plantarflexion angle at late stance period compared to that of the natural ankle), which validated the repeatability of the prosthesis

in different environment and configuration. However, the result of the prosthetic leg reached to its peak value at almost the same time with the result of healthy leg because the amputated and healthy legs should keep the same pace at walk. The ankle angle profile of the healthy leg showed a proper plantarflexion angle in late stance period, which indicated that the subject have a normal walking pattern and the reason for the small plantarflexion angle came from the prosthetic design (discussed later). The profiles of healthy leg and prosthetic leg all had a 10% time delay to the human ankle, this may be caused by personal walking habit and it could affect the overall performance of the prosthetic leg.

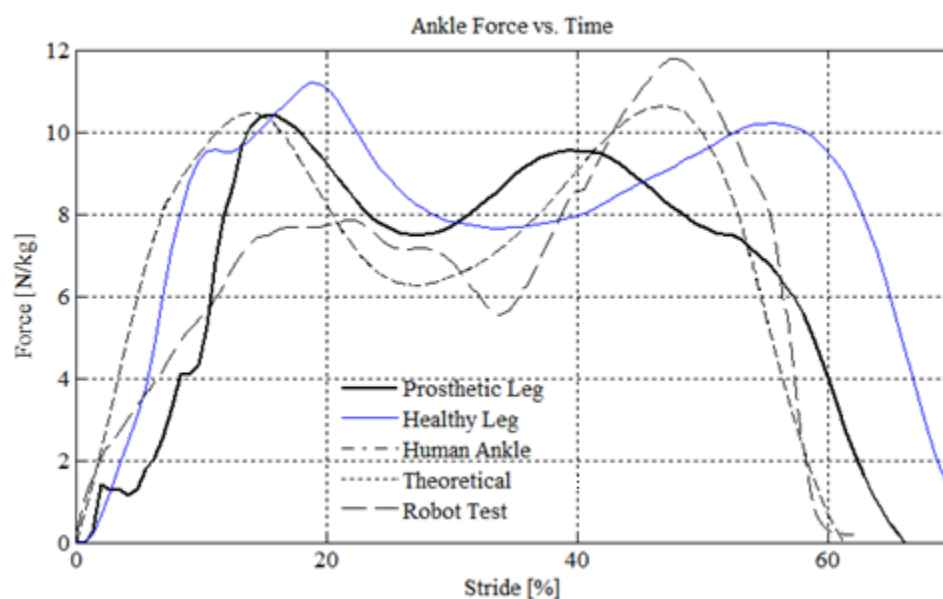


Figure 4.8 The Average Ankle Force for Human Subject Test and Comparisons

In Figure 4.8, the ankle force profile of the prosthetic leg appeared a similar shape with that of the human ankle, except that the interval between the two peaks was 8.4% smaller. The first peaks occurred at almost the same time with the same value, however, the difference between the second peaks was 1.3 N/kg (less than 10%).

As shown in Figure 4.9, the torque profile of the prosthetic leg had a similar tendency with the healthy leg. Although no plantarflexion angle was observed during push-off, the ankle torque reduced linearly. It was because a faster reductions of the ankle

angle and ankle torque occurred during push-off and the influence of the plantarflexion ankle torque (generated by the plantarflexion ankle angle at late stance period) was replaced. The peak value of the theoretical result, the robot test result and the prosthetic leg result were almost the same, which proves the accuracy of the optimization and the effect of the ankle deflection (the occurrences of peak ankle angles correspond to that of peak ankle torques).

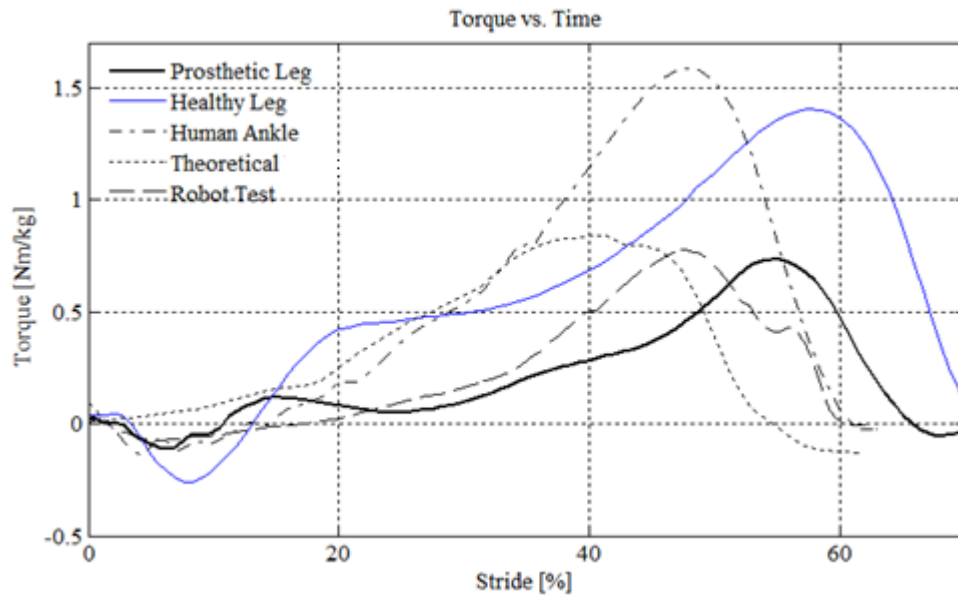


Figure 4.9 The Average Ankle Torque for Human Subject Test and Comparisons

Figure 4.10 shows the torque-angle relationships of the average result of human subject tests and other related results. It can be observed that the healthy leg of the human subject works similar to the average human ankle. No energy was dissipated at the healthy subject leg and the energy generated by the ankle (A_H , the lined area) was $0.124 J/kg$ per gait cycle. In this case, the total energy dissipated of the healthy leg was $-0.124 J/kg$ per gait cycle. As to the result of the prosthetic leg, no energy was generated and the total energy dissipated per gait cycle ($C_P = B_P$, the shaded area) was $0.103 J/kg$ per gait cycle. The difference of total dissipated energy between prosthetic leg in human subject testing and the theoretical result was $0.092 J/kg$ per gait cycle, which means that the prosthetic ankle in human subject tests dissipated more energy than the theoretical ankle.

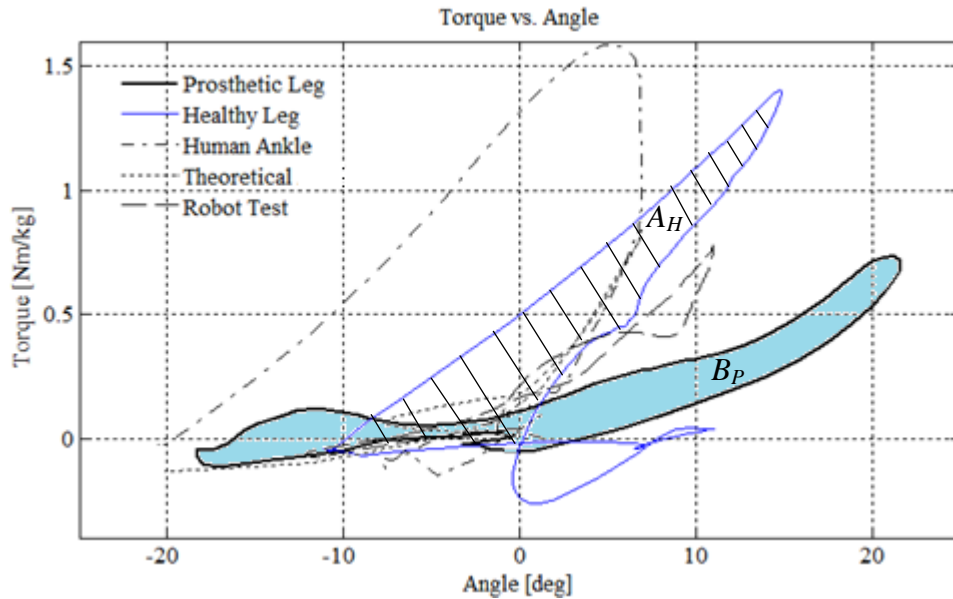


Figure 4.10 The Average Ankle Torque-Angle Relationship for Human Subject Test and Comparisons

4.2.3 Conclusion

The testing of the ankle prosthesis in a real environment was not as good as that tested on the robot. That is because that the situation of human subject testing is more complicated. For instance, the prosthesis had 3-dimensional movements when the human subject walked. Although we gave the subject time to adjust to the designed ankle prosthesis, it is far from enough for a patient to get used to a totally new device. The robot testing was performed in a totally controllable situation (the walking speed and the walking trajectory), thus the inputs and operation environment were almost the same for each trial. The inputs of subject testing, however, were unknown. Besides, the subject may change the walking trajectory to adjust the new device for each trial. A slight difference in body trajectory or walking speed could affect the performance of the prosthesis and reflect on the testing results.

The results of both the robot testing and the human subject testing showed that the ankle prosthesis could obtain the designed ankle motion, however, they also indicated that the prosthesis had a deficiency in controlling the relationship between the ankle

torque and the ankle angle. Although the results of the robot testing showed that the designed prosthesis has the ability to obtain active behavior, it was not as stable as its mechanical behavior (the subject test result showed no active behavior). More energy was dissipated ($0.103 J/kg$ per gait cycle) in the human subject tests. Modifications need to be addressed to the prosthesis design in the future to obtain more active behavior.

CHAPTER 5

Conclusion and Future Work

This chapter presents conclusions of the overall prosthetic design and provides some recommendations for the future work to improve the performance of the prosthesis. Section 5.1 summarizes the design and its performance. Section 5.2 provides suggestions for a better design.

5.1 Conclusion

A novel passive ankle prosthesis with two DoF was built and tested in this research. The objective of this research is to design a proof-of-concept ankle prosthesis that performs in a way similar to that of a natural ankle. Compression springs are used to store and release energy to emulate the active behaviors of the human ankle. The full assembled prosthesis weighs 2.3 *kg*, has a height of 245 *mm* and a width of 90 *mm*. Its range of motion is [0, 30 °] in both dorsiflexion and plantarflexion.

Robot tests were performed on the fabricated prosthesis. However, this design iteration is suboptimal. A mistake in the optimization was found after the device was fabricated. The prosthesis design was optimized again with only spring rates as design variables. A better result can be obtained by changing both the geometry and spring rates of the mechanism. Despite this, the test results showed that the prosthesis can provide a walking mode similar with the human ankle. The test results of the ankle angle showed that the prosthesis successfully emulates the ankle range of motion in CP phase and CD phase. The limited ankle deflection in the PP phase, however, effected the ankle torque profile and the torque-angle relationship. The ankle force and ankle torque profiles matched the general tendencies of natural ankle behaviors.

The robot tests also provided insights to the deficiencies of the structural design. The reason why robot tests were conducted before the human subject test was that many

unexpected situations could happen during testing. In this design, a main problem revealed by the robot tests was that the prosthesis operates in a larger range of ankle deflection. It is important because the increased range of motion may cause new interferences between components and may damage the prosthetic ankle during testing if no revision is made. Another problem the robot tests found is that the unlock mechanism can hardly work at first because the upper-leg cannot keep parallel with the lower-leg, which made less force is applied to the unlock piece to release the spring k_{lock} . This problem can also damage the vertical shafts that connect the upper-leg and lower-leg. Leg Connections were designed to improve the alignment of the prosthesis. The prosthetic ankle performed much better after all the modifications and preliminarily proved the validations of the prosthetic design.

The results of the human subject test reveal results similar to that of the robot test. While the results did not provide perfect matches with the human ankle behaviors, they provided experimental validation that the designed prosthesis has the ability to mimic human ankle. Human subject testing also showed that the prosthesis can obtain a similar ankle deflection and ankle force during operation. Although the prosthesis did not provide enough torque during push-off, the test torque profile successfully emulates the nonlinearity and the single-peak curve profile of a natural ankle.

5.2 Future Work

As a proof-of-concept prototype, several limitations exist in the design. Future work will address weight and size reduction and the improvement of the prosthetic mechanical performance.

The first future work need to be completed is to obtain the optimal parameter values of the prosthesis. New springs will be selected and the structures will be modified, even redesigned according to the optimal results.

The second work is to increase the stability and the range of motion of the ankle prosthesis during operation. Although the results of the robot tests show that the prosthetic ankle has a good stability and repeatability, the human subject tests reveal that there still exists the space to improve. The width of the foot and shape of the heel have effects on the stability of the prosthesis. They should be redesigned to provide a more stable basis for the amputee and be fitted in conventional shoes. Besides, the stiffness of the toe joint should be increased to better emulate the function of human foot and to obtain larger plantarflexion angles during the PP phase.

As the prosthesis tends to experience a larger range of ankle deflection during operation, the design for the second prosthetic iteration should take this into consideration. The increase range of motion can cause more interferences and even change the selection of springs. To avoid the problem, another motion simulation which uses the test result of this prosthetic design as benchmark should be performed. A redesigned structure with larger range of motion should be built in the next generation.

Despite weighting 2.3 kg remains in the acceptable range and the amputee subject stated that the weight of the prosthesis did not bother him at all, one of the main future work is to reduce the weight of the designed prosthesis. There are several ways to reduce the overall weight of the prosthesis. The majority of the weight locates in the stainless steel components. It is proved that some of them are unnecessary. For example, the pyramid adapter that used to connect the prosthesis to the residual limb can be made of titanium or aluminum instead of stainless steel. In the consideration of low friction, most of the moving components are made of stainless steel, including some big parts. In the second design, they could be made of a lighter material with stainless steel tubes inserted around the moving area.

With this design as a reference, the next iteration of the prosthetic design should be smaller, lighter and provide adequate ankle torque to the amputees. Active behavior is also an important function that the next design should achieve.

REFERENCE

- [1] Kim M. Norton. *A Brief History of Prosthetics*. inMotion Volume 17, Issue 7, November/ December 2007
- [2] K Graham, E.J. MacKenzie, P.L. Ephraim, T.G. Trivison, and R. Brookmeyer. *Estimating the Prevalence of Limb Loss in the United States: 2005 to 2050*. Archives of Physical Medicine and Rehabilitation 89(3):422-9. 2008.
- [3] L.E. Pezzin, T.R. Dillingham and E.J. MacKenzie. *Limb amputation and limb deficiency: Epidemiology and recent trends in the United States*. Southern Medical Journal, 95(8), August 2002.
- [4] M. W. Whittle. *Gait Analysis: An Introduction*, 4th ed. Elsevier Ltd: Butterworth-Heinemann, 2007.
- [5] David.A. Winter. *Biomechanics and motor control of human movement*. Wiley-Interscience, 1990.
- [6] Mitchell M.D. *Design and development of an intelligent ankle-foot prosthesis*. University of New Brunswick (Canada), 2007.
- [7] Samuel K. Au, Peter Dilworth, and Hugh Herr. *An ankle-foot emulation system for the study of human walking biomechanics*. IEEE International Conference on Robotics and Automation. Orlando, Florida. 2006
- [8] Brian J. Hafner, Joan E. Sanders, Joseph M Czerniecki, and Join Fergason. *Transtibial energy-storage-and-return prosthetic devicesL A review of energy Concepts and a proposed nomenclature*. Journal of Rehabilitation Research and Development, 39(1): 1-11. January 2002.
- [9] Bryan.J. Bergelin. *Design of a transtibial prosthesis utilizing active and passive components in conjunction with a four-bar mechanism*. M.S thesis, Marquette University, Milwaukee, WI, August 2010.
- [10] A.H. Hansen, D.S. Childress, S.C. Miff, S.A. Gard, and K.P. Mesplay. *The human*

- ankle during walking: implications for design of biomimetic ankle prostheses.*
Journal of Biomechanics, 37:1467–1474, 2004
- [11] Ryan D. Bellman, Matthew A. Holgate, and T. G. Sugar. *SPARKy 3: design of an active robotic ankle prosthesis with two actuated degrees of freedom using regenerative kinetics.* International Conference on Biomedical Robotics and Biomechatronics. Scottsdale, AZ. 2008
- [12] J. Hitt, T. Sugar, M. Holgate, R. Bellman, K. Hollander, *Robotic transtibial prosthesis with biomechanical energy regeneration.* Industrial Robot: An International Journal, 36(5): 441-447, 2009.
- [13] J.K. Hitt, T.S. Sugar, M. Hogate, and R. Bellman. *An active foot-ankle prosthesis with biomechanical energy regeneration.* Journal of Medical Devices, 4(1), March 2010.
- [14] IWALK Presents World’S First Actively Powered Foot And Ankle. 01/2010.
[online] uRL <http://singularityhub.com/2010/01/20/>
- [15] S. Au, J. Weber, and H. Herr. Powered ankle-foot prosthesis improved walking metabolic economy. IEEE Transaction on Robotics, 25(1), pp. 51-66.
- [16] Jingming Sun. Powered transtibial prosthetic device control system design, Implementation and testing. MS Thesis, Marquette University, Milwaukee, WI, August 2012
- [17] S. H. Collins and A. D. Kuo. *Recycling Energy to Restore Impaired Ankle Function during Human Walking.* PLoS ONE 5(2): e9307. 2010
(doi:10.1371/journal.pone.0009307)
- [18] [online] Active vs. Passive, uRL
http://www-personal.umich.edu/~kzelik/Active_vs_Passive_Devices.html
- [19] Shuguang Huang and Joseph M. Schimmels. Design of a 2 DoF prosthetic ankle using coupled compliance to increase ankle torque. International Design

- Engineering Technical Conferences & Computers and Information in Engineering Conference. Chicago, Illinois. 2012
- [20] Joseph K. Hitt, Ryan Bellman, Matthew Holgate, Thomas G. Sugar, and Kevin W. Hollander. *The SPARKy (Spring Ankle With Regenerative Kinetics) Project: Design and Analysis of a Robotic Transtibial Prosthesis With Regenerative Kinetics*. ASME Conf. Proc. 2007, 1587 (2007).
- [21] [online] NX: Siemens PLM Software, uRL.
http://www.plm.automation.siemens.com/en_us/products/nx/
- [22] [online] Friction and Coefficients of Friction, uRL.
http://www.engineeringtoolbox.com/friction-coefficients-d_778.html
- [23] [online] Miniature High-Precision Stainless Steel Ball Bearings
<http://www.mcmaster.com/#standard-ball-and-roller-bearings/=kh93ft>
- [24] [online] DryLin® R - Linear plain bearing RJUM-01
http://www.igus.com/wpck/default.aspx?pagename=drylin_r_rjum_01
- [25] Robert Norton. *Design of Machinery*. McGraw-Hill, 2003.
- [26] Richard G. Budynas and J. Keith Nisbett. *Shigley's mechanical engineering design*. McGraw-Hill, 2011.
- [27] ATI Industrial Automation. *F/T Controller (CTL / CTLJ / CON), Six-Axis Force/Torque Sensor System Compilation of Manuals*. March 2012.

APPENDIX A

Prosthetic Detailed Design Considerations

A.1 Prosthetic Mechanical and Material Properties

The mechanical properties for aluminum 6061, ABS plastic, stainless steel 103 and 106 are presented in Tables A.1.1 – A.1.3.

Table A.1.1 Properties of Aluminum 6061 T6

Properties	Metric Value
Density	2.7 g/cm ³
Hardness, Rockwell B	60
Modulus of Elasticity	68.9 GPa
Tensile Yield Strength	276 MPa
Fatigue Strength	96.5 MPa
Shear Strength	207 MPa

Table A.1.2 Properties of ABS Plastic

Properties	Metric Value
Density	1.05 g/cm ³
Hardness, Rockwell	R105
Modulus of Elasticity	1.627 GPa
Tensile Yield Strength	22 MPa
Flexural Strength	41 MPa

Table A.1.3 Mechanical Properties for Stainless Steel

Stainless Steel	Density (g/cm ³)	Tensile Strength (Mpa)	Yield Strength (Mpa)	Reduction of Area	Elongation in 2"	Brinell Hardness
303	7.9	620	240	50-60	45-55	160-180
316	8.03	690	200	50	40	180

Figure A.1.1 shows spring configurations for spring sets k_2 , k_{s1} and k_{s2}/k_{s3} during their equilibrium position, maximum dorsiflexion position and maximum plantarflexion position. The circles represent the connection positions. All values are in *mm*.

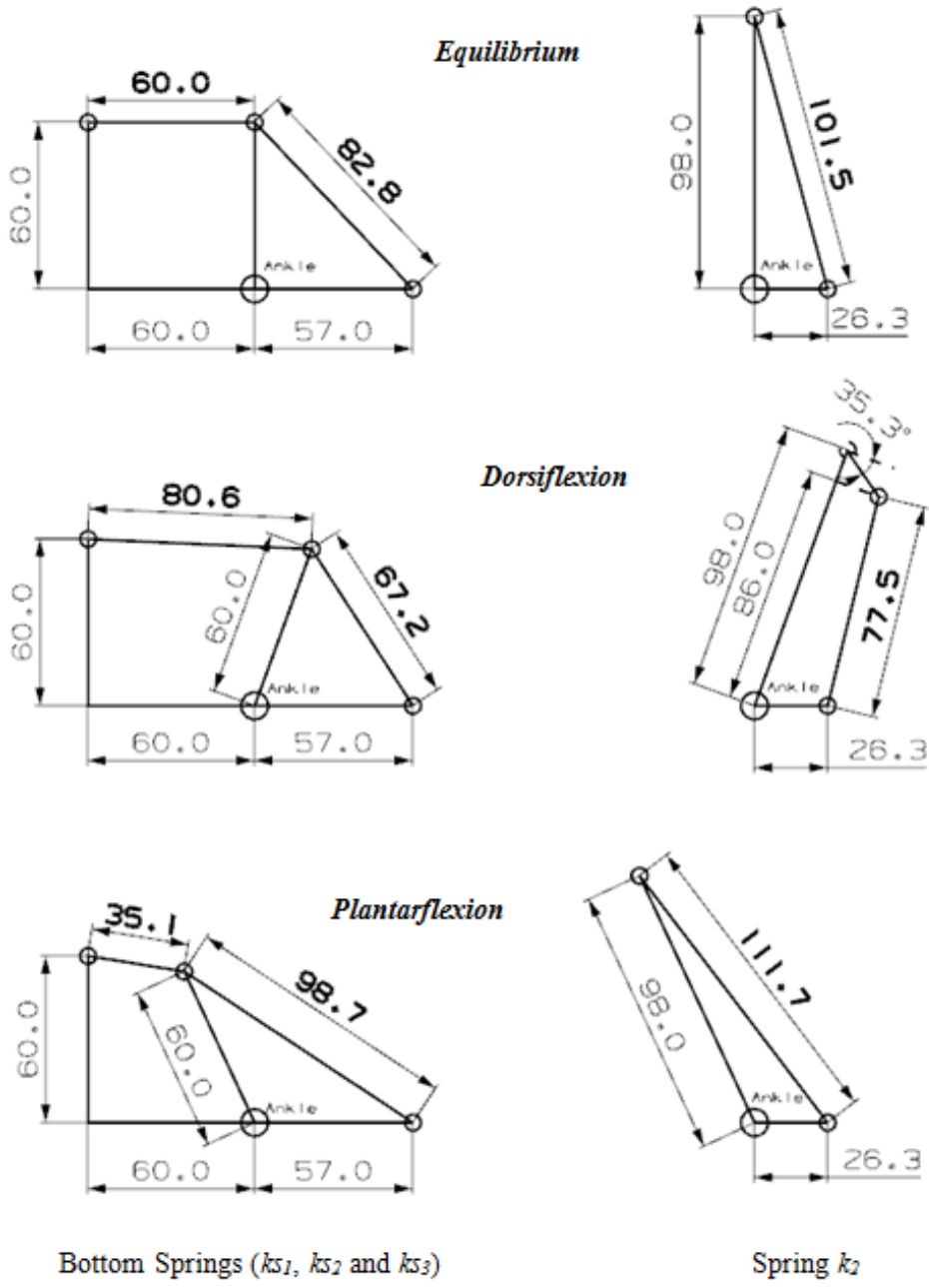


Figure A.1.1 Spring Configurations for Spring Sets k_2 , k_{s1} and k_{s2}/k_{s3}

Figure A.1.2 shows the models and dimensions for the ball bearings and linear bearings chosen in this design. The sizes and mechanical properties of the selected models are shown in Table A.1.4 and Table A.1.5.

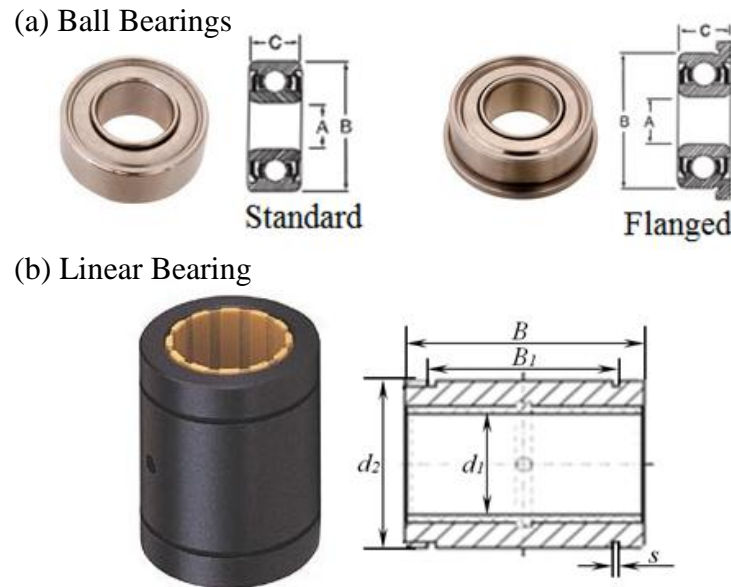


Figure A.1.2 Dimensions for Ball Bearings and Linear Bearing

Table A.1.4 Properties for Conventional Ball Bearings from *McMaster* [24]

Bearing	A (mm)	B (mm)	C (mm)	Dynamic Radial Load Cap. (N)	Max rpm
7804K111	6	10	3	500	53,000
7804K112	6	12	4	712	50,000
7804K113	6	13	5	1080	48,000
7804K147	8	16	5	1250	43,000

Table A.1.5 Properties of Linear bearing from *IGUS* [25]

Bearing	$d1$ (mm)	$d2$ (mm)	B (mm)	$B1$ (mm)	s (mm)	F max. Dynamic (N)	F max. Static (N)	Weight (g)
RJZM-01-08	8	16	25	16.2	1.1	960	6720	9

A.2 Prosthetic Fabrication Figures and Tables

Table A.2.1 presents the quantities, materials and prices for all designed components. Table A.2.2 shows the quantities and prices for all standard components that the ankle prosthesis needed.

Table A.2.1 Fabrication Cost of Prosthesis Components

Parts Name	Quantity	Material	Price
Lower Leg	1	Aluminum 6061	\$150
Up Leg	1	Aluminum 6061	\$350
BaseFoot-1	1	Aluminum 6061	\$185
BaseFoot-2	1	Aluminum 6061	\$185
Shaft Connect-Wall	2	Aluminum 6061	\$110
Left Side Wall	1	Aluminum 6061	\$271
Right Side Wall	1	Aluminum 6061	\$271
Shaft-Walls	1	Aluminum 6061	\$93
Adapter	1	Stainless Steel 316	\$265
Shaft Ks-D1	2	Stainless Steel 316	\$220
Shaft Ks-D2	1	Stainless Steel 303	\$45
Shaft Ks-D3	1	Stainless Steel 316	\$220
Shaft Ks-L	1	Stainless Steel 316	\$315
Shaft Ks-H	1	Stainless Steel 303	\$115
Shaft K2-L	1	Stainless Steel 316	\$165
Shaft K2-L1	1	Stainless Steel 316	\$145
Shaft K2-D	1	Stainless Steel 303	\$225
Shaft K2-D1	1	Stainless Steel 316	\$120
Shaft K2-H	1	Stainless Steel 303	\$120
Shaft K back H push	2	Stainless Steel 303	\$420
Shaft K back H-1	1	Stainless Steel 316	\$270
Shaft K back H-2	2	Stainless Steel 316	\$110
Unlock pin	1	Stainless Steel 303	\$85
Unlock	2	Stainless Steel 316	\$190

Table A.2.1 Fabrication Cost of Prosthesis Components — Continued

Lock pin	2	Stainless Steel 303	\$220
Shaft K1-1	3	Stainless Steel 303	\$186
Shaft K1-2	3	Stainless Steel 316	\$90
Lock 2	2	Stainless Steel 303	\$570
Lock 1-L	1	Stainless Steel 316	\$910
Lock 1-R	1	Stainless Steel 316	\$910
Shaft K2-Sleeve	1	Stainless Steel 303	\$55
Shaft Connect-Lock	1	Stainless Steel 303	\$55
Total			\$7641

Table A.2.2 Prosthesis Bill of Materials

Quantity	Part Number	Description	Unit Price	Total Price
3	71482	Robot test spring $k_{1, front}$ from CSC	\$5.64	\$16.92
2	S-1129	Robot test spring $k_{1, back}$ from CSC	\$3.49	\$6.98
2	71825	Robot test spring k_2 from CSC	\$8.34	\$16.68
3	71497	Robot test spring k_{s1} from CSC	\$5.52	\$16.56
2	3057	Robot test spring k_{s2} from CSC	\$2.98	\$5.96
2	70973S	Robot test spring k_{s3} from CSC	\$6.48	\$12.96
4	S-1420	Spring k_{lock} from CSC	\$1.88	\$7.52
4	K-44	Spring k_{top} from CSC	\$1.99	\$7.96
3	3851	Subject test spring $k_{1, front}$ from CSC	\$2.64	\$7.92
2	K-56	Subject test spring $k_{1, back}$ from CSC	\$2.38	\$4.76
2	S-1332	Subject test spring $k_{2, top}$ from CSC	\$4.02	\$8.04
2	Q-75	Subject test spring $k_{2, bottom}$ from CSC	\$2.58	\$5.16
3	11390	Subject test spring k_{s1} from CSC	\$2.47	\$7.41
2	10416	Subject test spring k_{s2} from CSC	\$4.69	\$9.38
2	W-71	Subject test spring k_{s3} from CSC	\$2.15	\$4.30
3	RJZM-01-08	Linear bearing from IGUS	\$9.34	\$28.02
4	7804K111	Ball bearing for 6 mm ID, 10 mm OD	\$6.64	\$26.56
14	7804K112	Ball bearing for 6 mm ID, 12 mm OD	\$7.67	\$107.38
5	7804K113	Ball bearing for 6 mm ID, 13 mm OD	\$5.54	\$27.70

Table A.2.2 Prosthesis Bill of Materials — Continued

3	7804K147	Flanged ball bearing for 8 <i>mm ID</i> , 16 <i>mm OD</i>	\$7.15	\$21.45
1 (pack)	98317A217	Side-mount external ring for 8 <i>mm</i> shaft	\$7.20	\$7.20
1 (pack)	98541A112	External circlip for 4 <i>mm</i> shaft	\$4.95	\$4.95
1 (pack)	98541A114	External circlip for 6 <i>mm</i> shaft	\$5.71	\$5.71
1 (pack)	90296A409	Internal helical Insert M4, 6 <i>mm</i> length	\$7.84	\$7.84
1 (pack)	90296A302	Internal helical Insert M5, 7.5 <i>mm</i> length	\$7.02	\$7.02
1 (pack)	90296A306	Internal helical Insert M6, 6 <i>mm</i> length	\$6.67	\$6.67
1 (kit)	91732A944	Standard helical insert repair kit for M4	\$35.92	\$35.92
1 (kit)	91732A946	Standard helical insert repair kit for M5	\$35.51	\$35.51
1 (kit)	91732A948	Standard helical insert repair kit for M6	\$35.86	\$35.86
1 (pack)	92855A616	Metric socket cap screw M6 size, 16 <i>mm</i>	\$8.47	\$8.47
1 (pack)	92855A513	Metric socket cap screw M5 size, 12 <i>mm</i>	\$8.11	\$8.11
1 (pack)	92855A410	Metric socket cap screw M4 size, 10 <i>mm</i>	\$8.64	\$8.64
Total				\$529.14

APPENDIX B

Robot Testing Protocol and Results

B.1 Sensor Data Interpretation

Figure B.1.1 and Figure B.1.2 show the calibration profiles for the linear potentiometer and the rotary potentiometer. The data acquired by LabView is the voltage changes of the potentiometers. A 5 V voltage was applied to the potentiometers during the calibration and the robot testing.

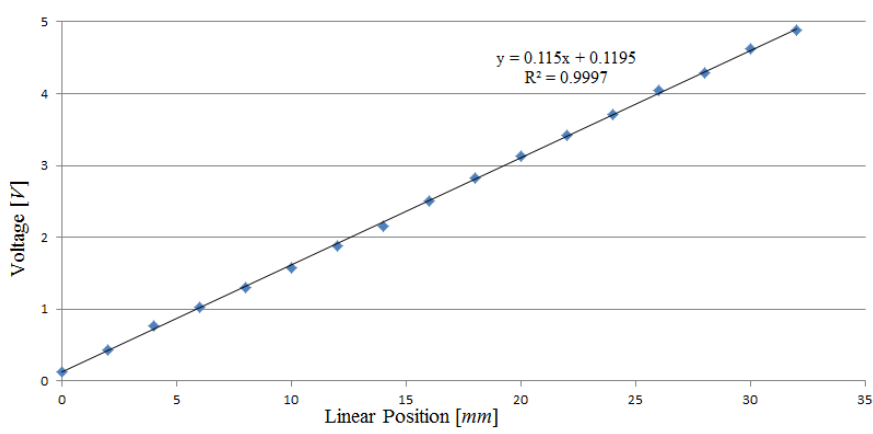


Figure B.1.1 Calibration curve for Linear Potentiometer

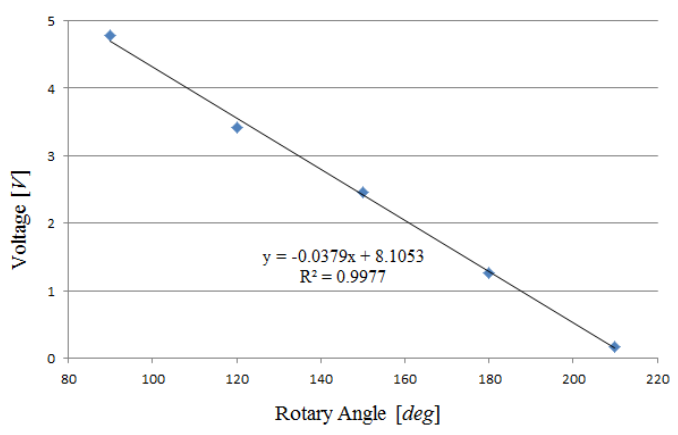


Figure B.1.2 Calibration Curve for Rotary Potentiometer

A Force/ Torque Sensor is used to acquire the force and torque data during robot testing. The data streams recorded by the F/T sensor are non-dimensional values. For the first three values, one count means $1/32 N$ and for the last three values, one count means $0.9 Nmm$. The data acquired by LabView is the voltage changes of the F/T sensor.

It is difficult to directly measure the force and torque at ankle joint J_0 because the sensor is instrumented at the top of the prosthesis during testing. The forces and torques of the top end of the prosthesis are measured instead. A transformation of the forces and moments are illustrated in Figure B.1.3. In the calculation, d represents the distance between point A and Point B; it changes during the operation of the prosthesis and the deflection is measured by the linear potentiometer.

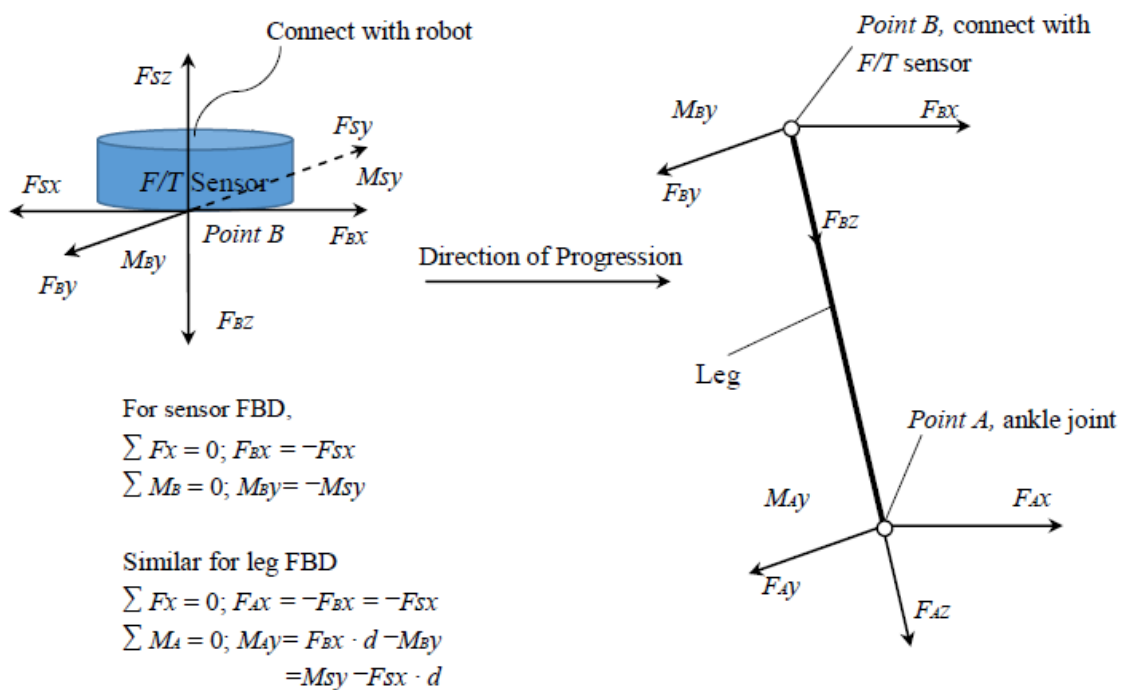


Figure B.1.3 Force and Torque Transformation of F/T Sensor

Figure B.1.4 shows the multiple trajectories of the top head of fibula of a natural human fibula joint during the stance period. They are obtained from the healthy leg of the human subject during testing. The average trajectory is used as initial controlling points for the robot testing.

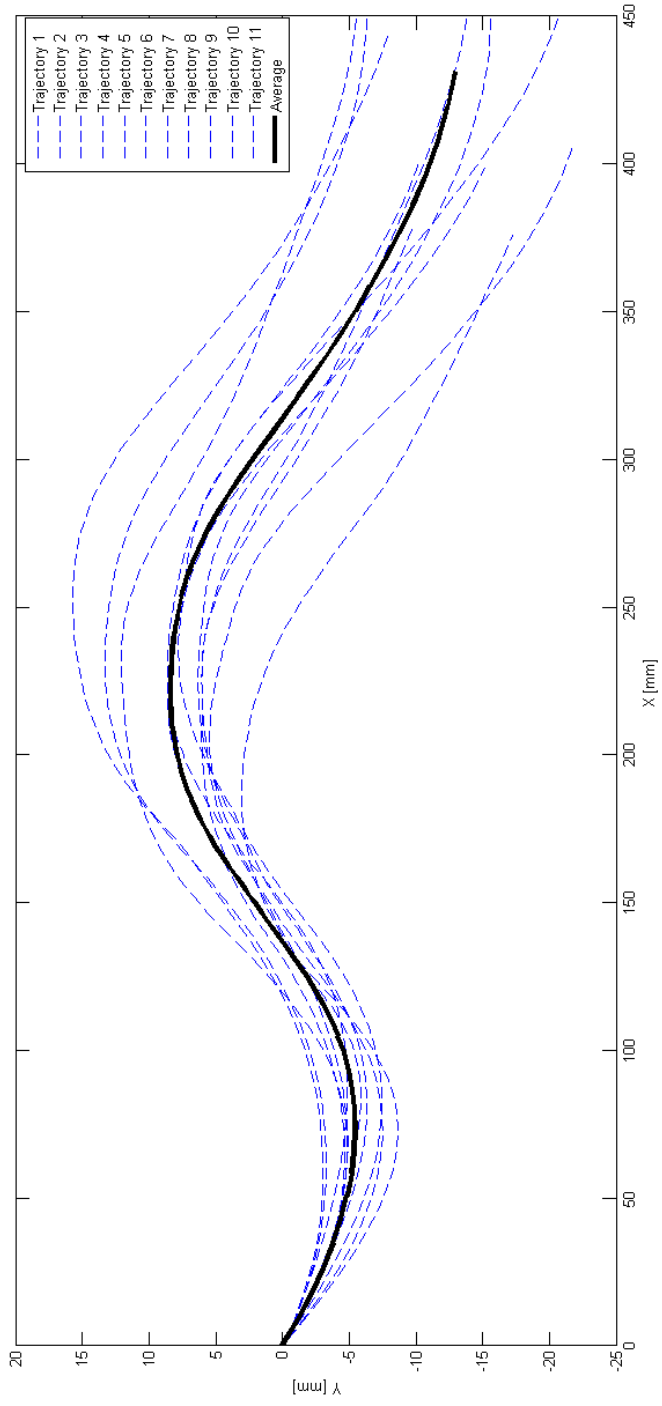


Figure B.1.4 Walking Trajectories of the Top Head of Fibula of a Natural Ankle

B.2 Robot Testing Protocol for Designed Prosthesis

1. Attach the assembled prosthesis to the robot. Make sure that the bottom of the prosthesis has no contact with the ground.
2. Power up the robotic controller, load the program (tib.1) that has already been stored in the robot disk and set the speed to 50 *mm/s* (or in the range of [35, 70]).
3. Power up computer and NI ELVIS. Open Hyper Terminal and the LabView Program
4. Open the *F/T* controller and Biasing the sensor using command 'SB'.
5. Enable power of the robotic arm and set a reference point to the robot.
6. When the prosthesis is ready to test, start data acquisition (using command 'QS' in Hyper Terminal and pressing 'run' button in LabView Program) and specify the file name and position that used to store the acquired data.
7. Give an output impulse to the prosthesis and then execute testing program in the robot.
8. After the robotic program ends, stop LabView programs and Hyper Terminal. Disable the power of the robotic arm if necessary.
9. Repeat steps 6 to 8 for next trial.
10. In case of emergency, a red E-stop button is available on the control panel.
11. Remember that although the nominal load of the robot is small, it can generate much bigger load when you type in a wrong position. Make sure that a slow 'empty load' run of each new trajectory program is conducted.

B.3 Robot Testing Results

In the following figures (Figure B.1.5 to Figure B.1.8), the robot test results are compared between each trail. Three parameters (the ankle angle, the ankle torque and the force along the leg) are used in the comparison. It can be observed that the test results are very close to each other. The curves of the force profile and the torque profile have the typical shapes similar to that of human ankle. Although the torque-angle relationship did not match the human ankle behavior very well, a nice nonlinearity and a small amount of active behavior are observed.

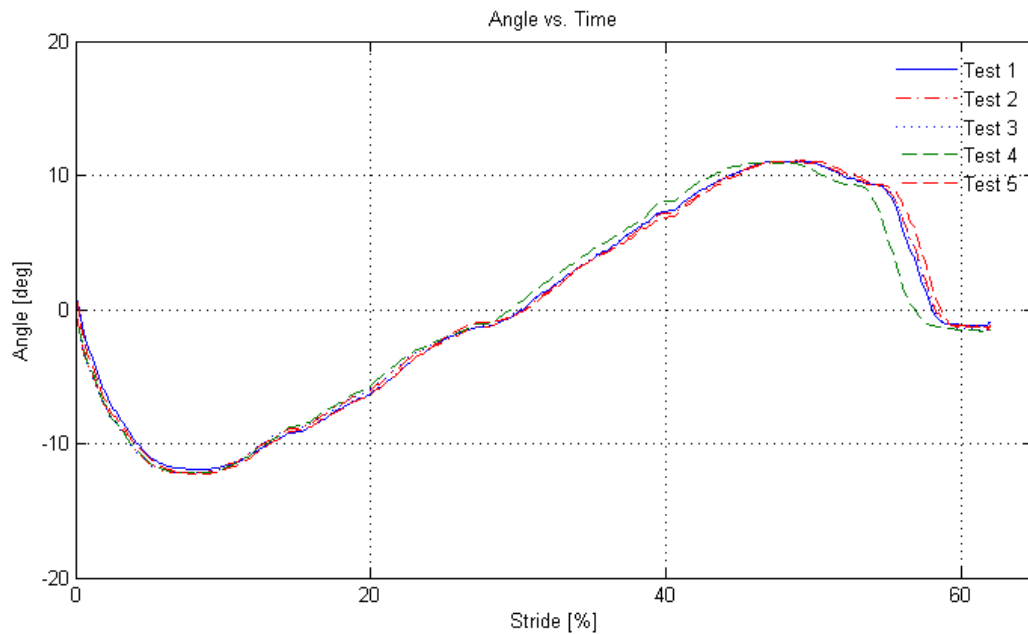


Figure B.1.5 The Ankle Angle Profiles for Each Robot Test Trial

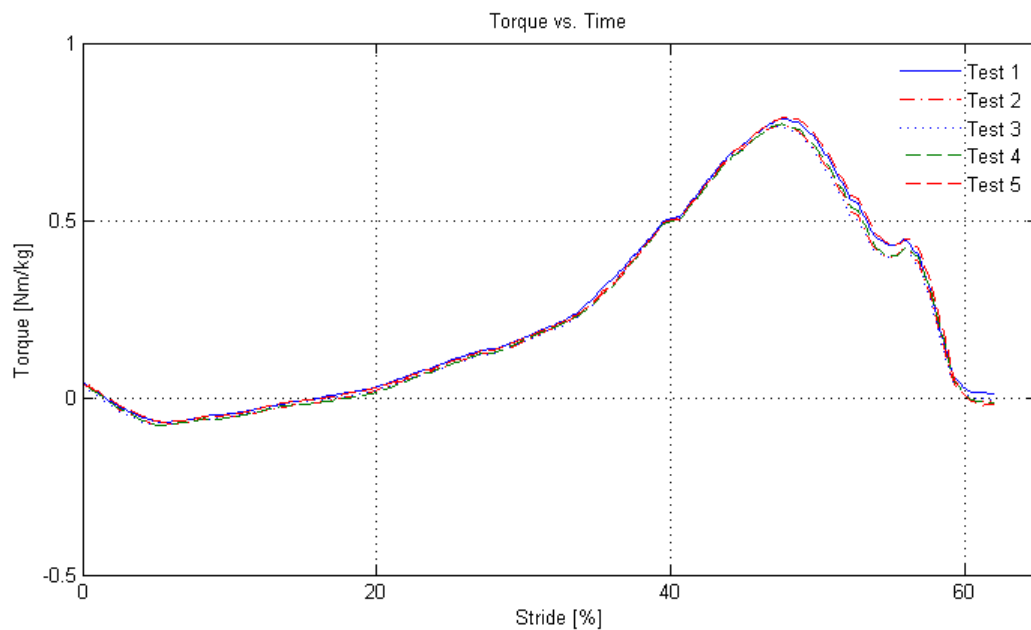


Figure B.1.6 The Ankle Torque Profiles for Each Robot Test Trial

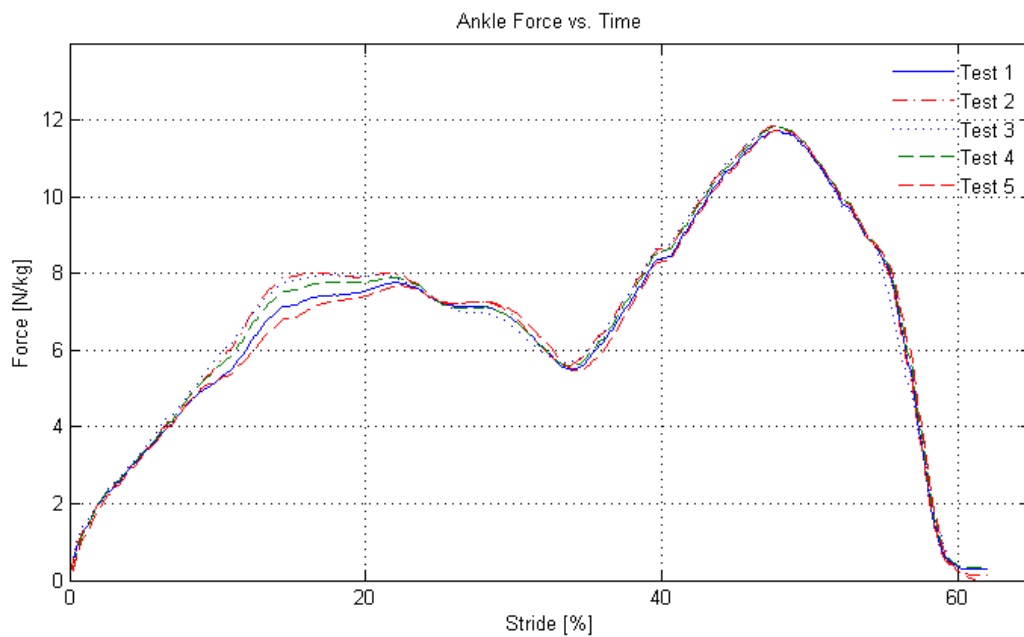


Figure B.1.7 The Ankle Force Profiles for Each Robot Test Trial

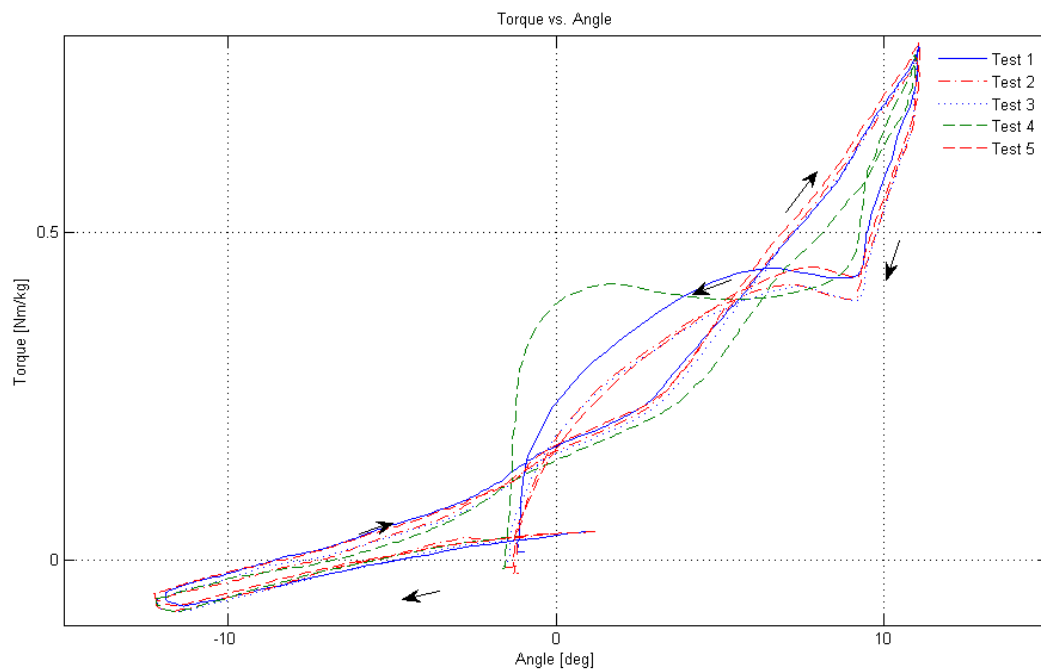


Figure B.1.8 The Torque-Angle Relationship Profiles for Each Robot Test Trial

APPENDIX C

Human Subject Testing Results

In Figure C.1.1 to Figure C.1.4, the comparisons of selected parameters (ankle angle, ankle torque and force along the leg) between each successful human subject test trial are shown. The curves for the angle and force were very close to each other. The time to obtain the peak values of the torque profile were a little different because of the effects of the environment and the slightly changes in the walking pattern of the subject.

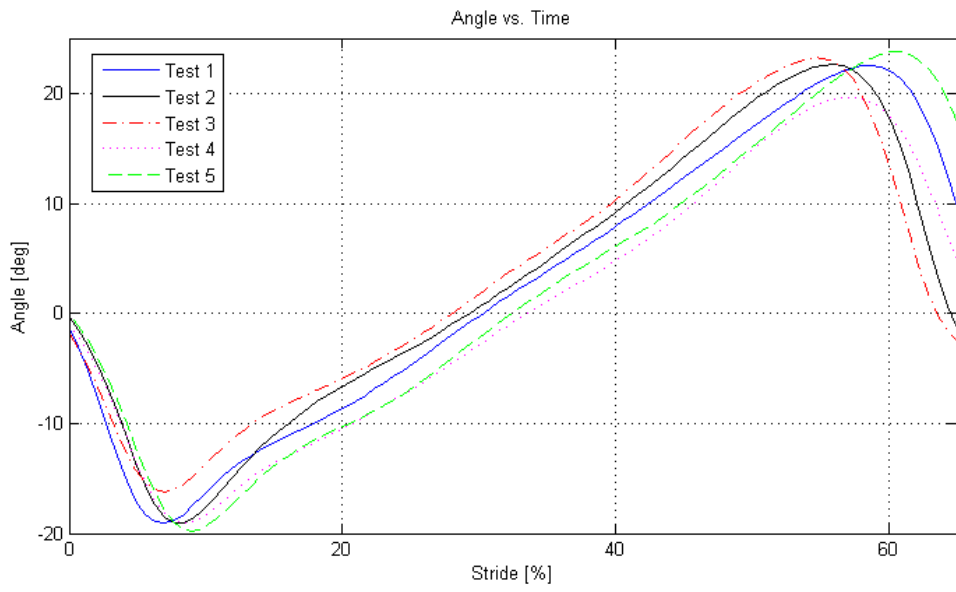


Figure C.1.1 The Ankle Angle Profiles for Each Human Subject Test

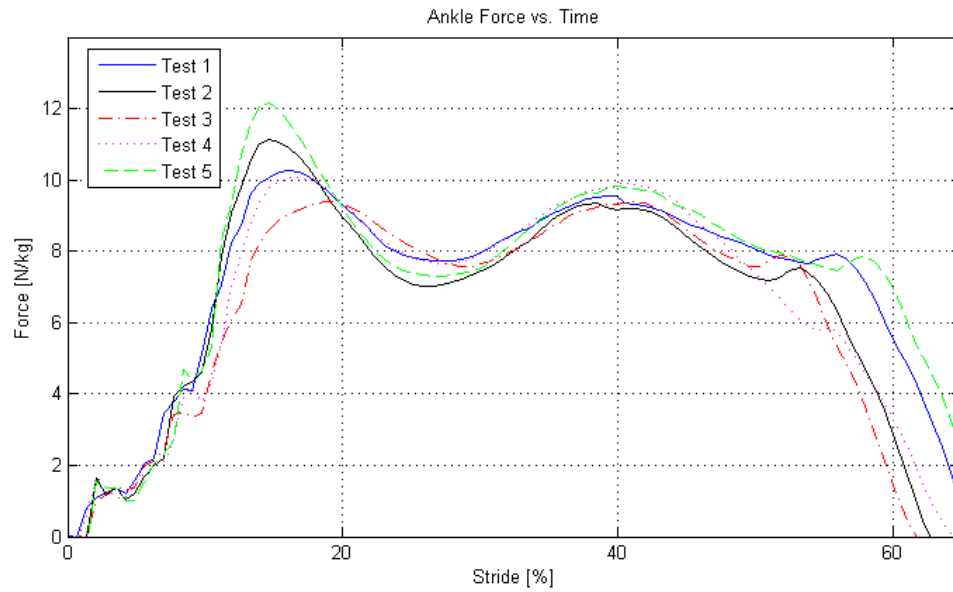


Figure C.1.2 The Ankle Force Profiles for Each Human Subject Test

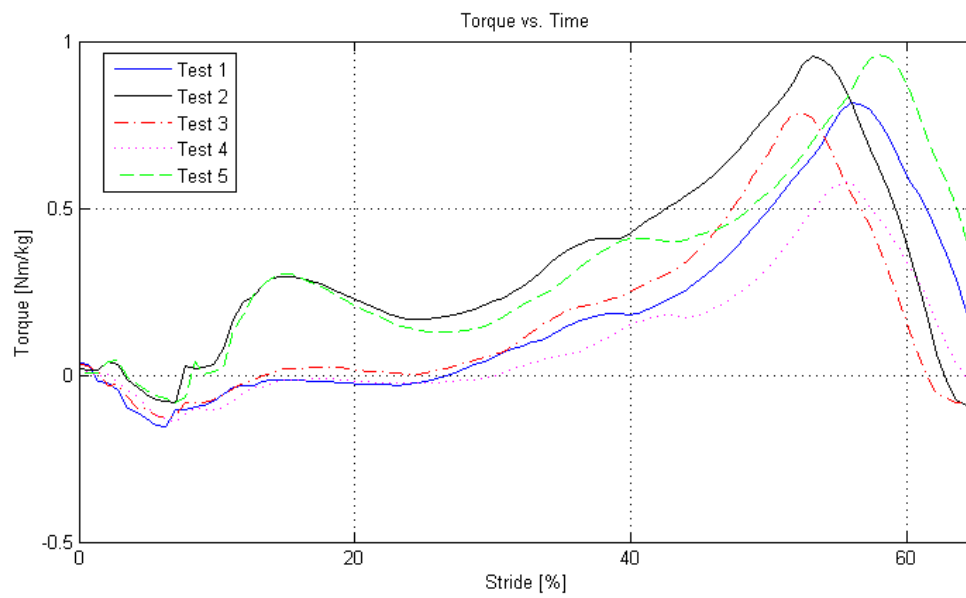


Figure C.1.3 The Ankle Torque Profiles for Each Human Subject Test

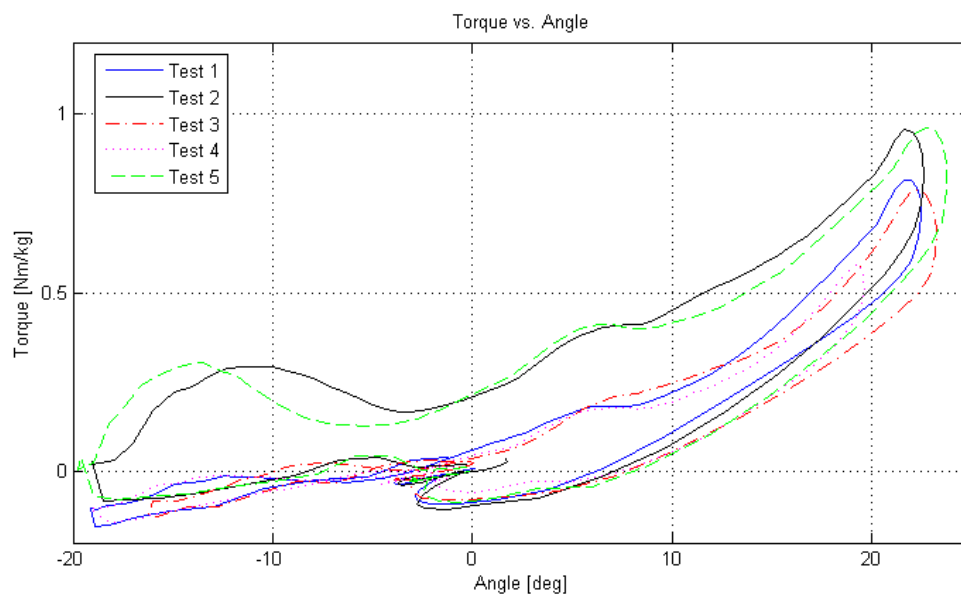


Figure C.1.4 The Torque-Angle Relationship for Each Human Subject Test